NASA Contractor Report 4147

Turbofan Forced Mixer Lobe Flow Modeling

II—Three-Dimensional Inviscid Mixer Analysis (FLOMIX)

T. Barber

CONTRACT NAS3-23039
OCTOBER 1988

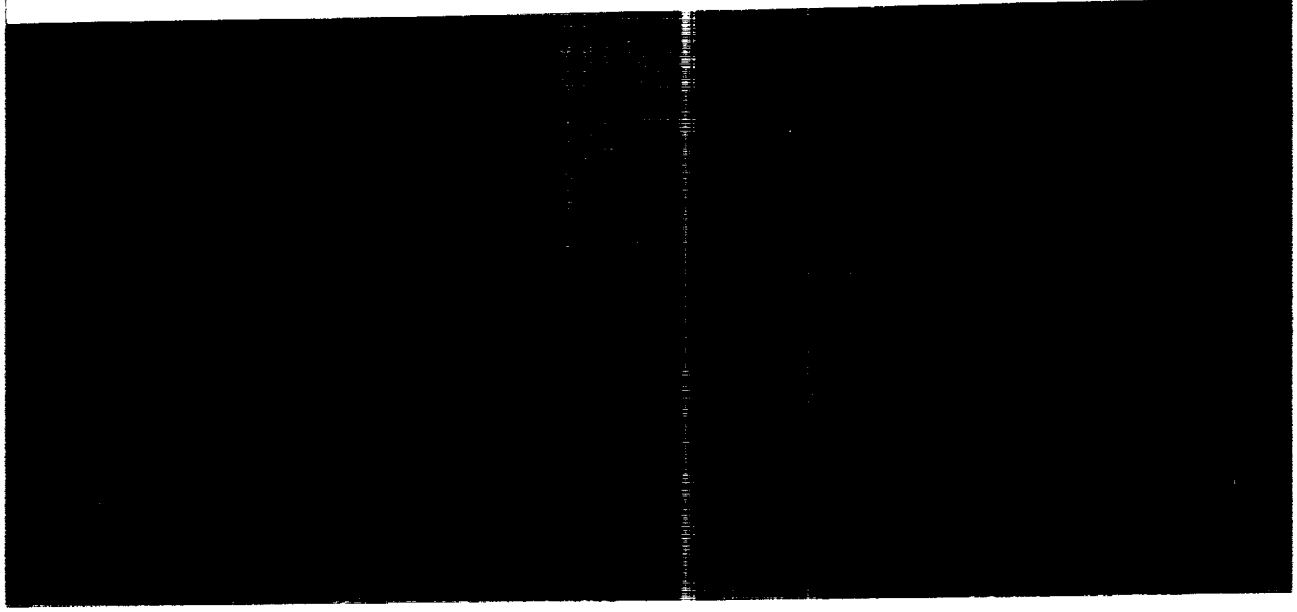

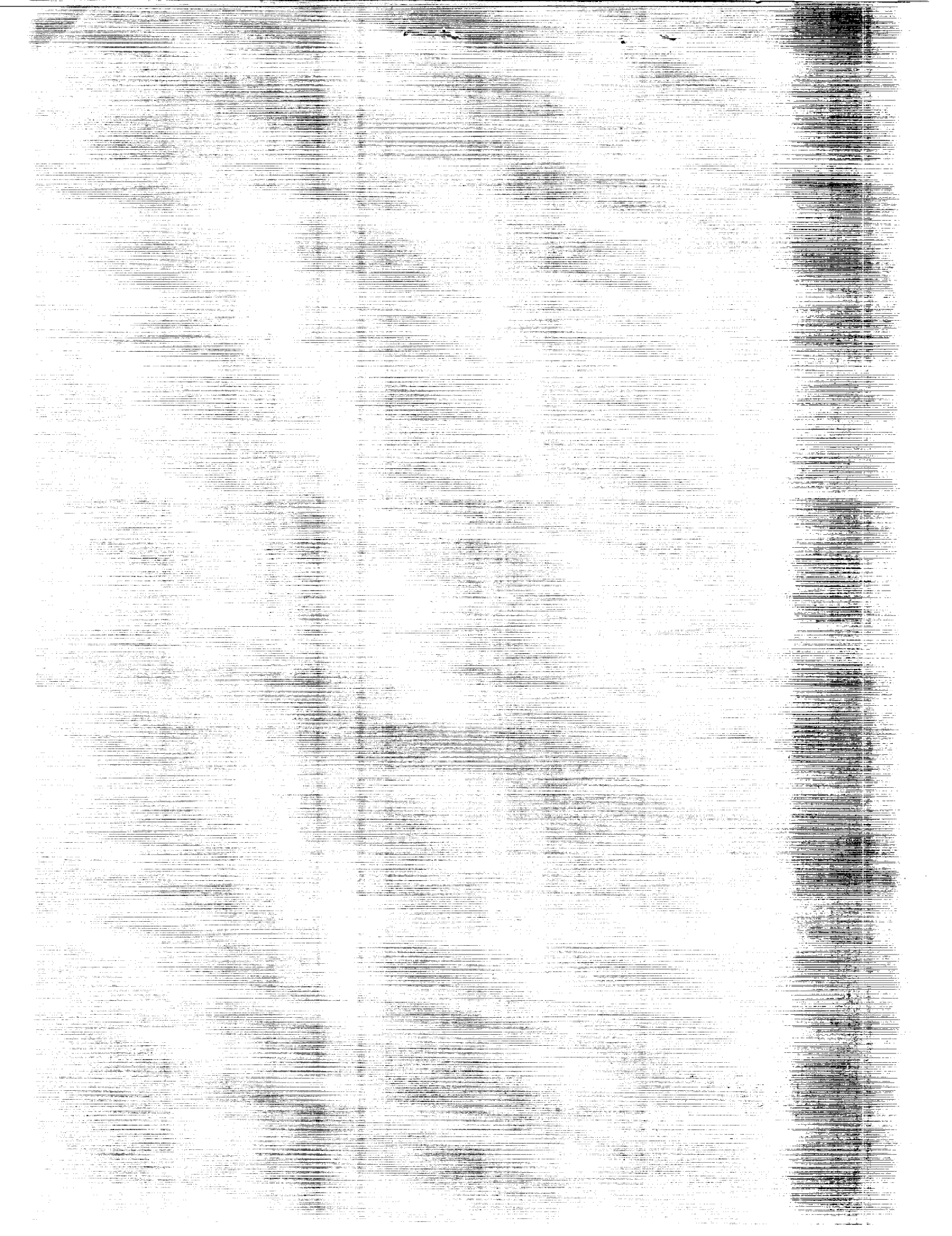

NASA Contractor Report 4147

Turbofan Forced Mixer Lobe Flow Modeling

II—Three-Dimensional Inviscid Mixer Analysis (FLOMIX)

T. Barber
United Technologies Corporation
Pratt & Whitney Engineering Division
East Hartford, Connecticut

Prepared for
Lewis Research Center
under Contract NAS3-23039

National Aeronautics
and Space Administration

Scientific and Technical
Information Division

1988

FOREWORD

The overall objective of this NASA program has been to develop and implement several computer programs suitable for the design of lobe forced mixer nozzles. The approach consisted of extending and existing analytical nacelle analysis to handle two stream flows where one of the streams is at a higher energy. Initially the calculation was set up to handle a round, free mixer including satisfying the Kutta condition at the trailing edge of the mixer. Once developed and calibrated, the same analysis was extended to handle periodic boundary conditions associated with typical engine forced mixers. The extended analysis was applied to several mixer lobe shapes to predict the downstream vorticity generated by different lobe shapes. Data was taken in a simplified planar mixer model tunnel to calibrate and evaluate the analysis. Any discrepancies between measured secondary flows emanating downstream of the lobes and predicted vorticity by the analysis is fully reviewed and explained. The lobe analysis are combined with an existing 3D viscous calculation to help assess and explain measured lobed data.

The program also investigated technology required to design forced mixer geometries for augmentor engines that can provide both the stealth and performance requirements of future strategic aircraft. For this purpose, UTC's available mixer background was used to design several preliminary mixer concepts for application in a exhaust system. Based on preliminary performance estimates using available correlations, two mixer configurations will be selected for further testing and analysis.

The results of the program are summarized in three volumes, all under the global title, "Turbofan Forced Mixer Lobe Flow Modeling". The first volume is entitled "Part I - Experimental and Analytical Assessment" summarizes the basic analysis and experiment results as well as focuses on the physics of the lobe flow field construed form each phase. The second volume is entitled "Part II - Three Dimensional Inviscid Mixer Analysis (FLOMIX)". The third and last volume is entitled "Part III - Application to Augmentor Engines".

TABLE OF CONTENTS

SECTION 1.0
INTRODUCTION

A forced mixer is a device that is used on gas turbine engines to internally mix the hot turbine efflux with the cooler, lower velocity fan bypass or secondary stream. The principle motivator for doing this on commercial gas turbine engines is to reduce the jet noise associated with the high energy core stream. Also, when designed properly, the mixer can also achieve an increase in gross thrust while realizing noise reductions. Figure 1 shows a typical separate and mixed flow nacelle. Note that to achieve the mixing, the duct surrounding the engine must be lengthened. This adds weight, as does the mixer and the larger centerbody plug. Normally, and particularly for short range aircraft applications, these weight penalties offset the thrust improvements. In addition, the increased difficulty of intergrating the longer nacelle into the aircraft flow field without incurring interference drag penalties, in the past has prevented launching new engines into service as mixed flow nacelles purely on a performance basis. However, with increasingly stringent noise regulations, mixers are being considered for future commercial engine applications. Mixers are also being considered in military applications as variable area devices for varying cycle match and as a way of spreading the hot turbine exhaust ahead of afterburning flameholders. This report presents an analytical method which has been developed for the mixer lobe flowfield.

SEPARATE FLOW NACELLE

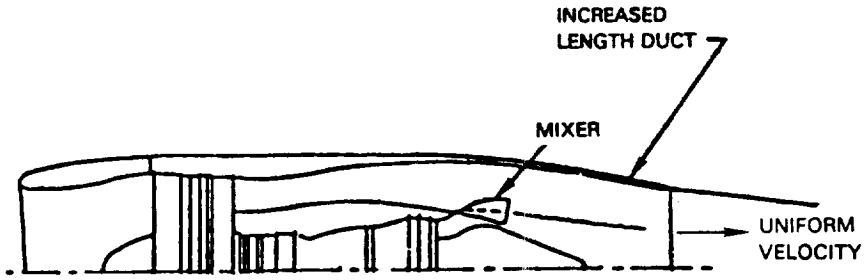

MIXED FLOW NACELLE

Figure 1 Typical Nacelle Exhaust Configurations

Conventional or commercial forced mixer geometries consist of periodic lobe structure that can be described in terms of a number of geometric features. Figure 2 illustrates two cross-sectional views of the lobe. The scarf angle or lobe cutback angle is used to reduce lobe length with increasing penetration into the core. Scalloping is a cutout of the lobe lateral surface used to minimize lobe wall structural problems while promoting tangential mixing.

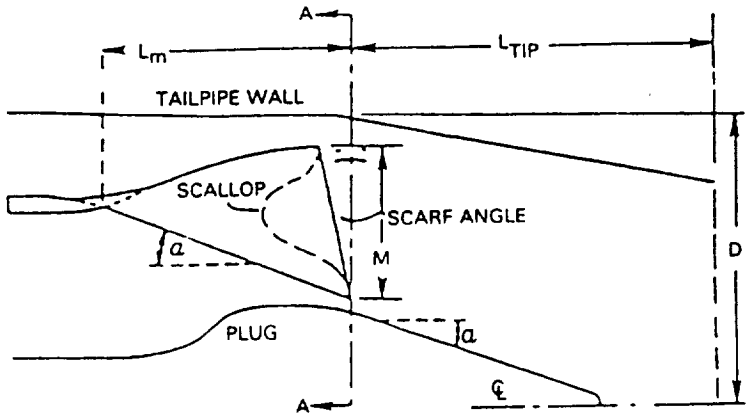

a) SECTION B-B

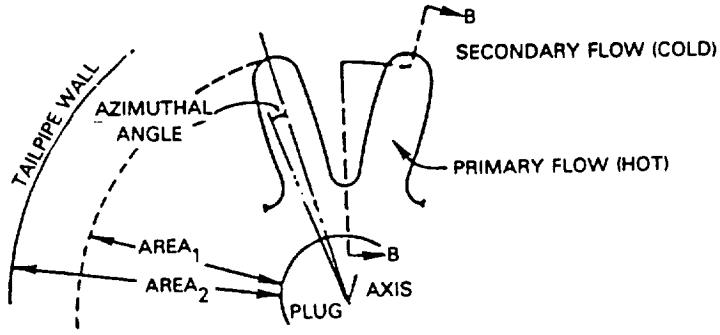

b) SECTION A-A

Figure 2 Mixer Lobe Geometry Definition

For many years the mixer was designed using a trial and error experimental approach, wherein limited traverse and performance data was used to refine design concepts. [1-3] More recently, "benchmark" experiments [4,5] resorting to high response and LDV instrumentation have probed the mixing chamber in an attempt to explain the mixing process and its driving mechanisms. These experiments confirmed that the mixing process is a viscous dominated process, [6] and that the primary driving mechanism is the secondary flows generated in the lobed region of the flow. Several researchers have proposed a variety of inviscid and viscid processes for producing the secondary flow, but as yet, no attempt has been made to analytically model them. Anderson and Povinelli [7,8] have lumped these terms together under a "gereric" vorticity label, analytically simulating its effect in terms of a vortex sheet distributed along the lobe exit surface. Such an approach has been used to generate inlet conditions for a viscous marching analysis in the mixing duct. The results of these calculations, as seen in Figure 3, have been shown to realistically simulate observed flow mixing patterns. The purpose of this paper is to develop an inviscid analysis which, in conjunction with a lobe boundary layer analysis, can predict the flow over the mixer lobes, thereby obtaining the conditions needed to initiate a marching viscous calculation in the downstream duct.

The analysis presented in this report is an attempt to examine one particular inviscid secondary vorticity generator called the "flap" vorticity scheme (Figure 4). In this model, the vorticity is associated with the periodic lift distribution produced by the periodic lobe trailing edge. The feasibility of an inviscid method predicting an observed level of flow penetration is dependent on the axial flow component remaining attached to the surface. Surface pressure and shed vorticity distributions will therefore be examined to calibrate the method.

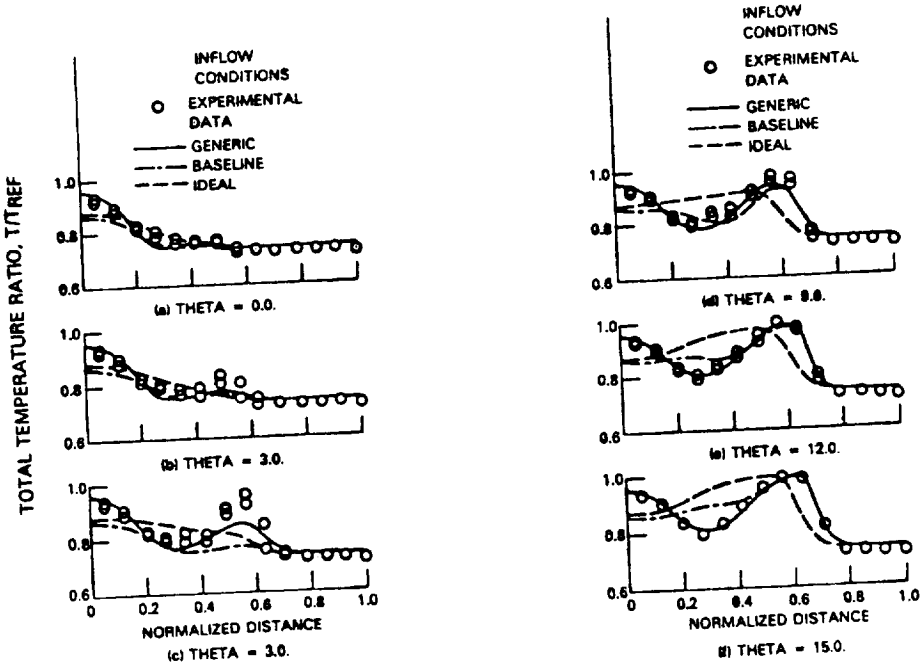

Figure 3 Comparison of computed temperature profiles with experimental data, Case 12C Mixer, T_f/T_c = 0.74, Station 21.

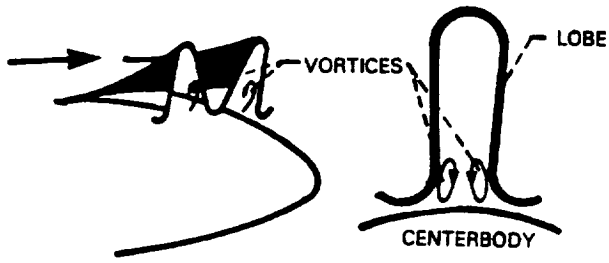

SECONDARY FLOW GENERATION, PASSAGE VORTEX

Figure 4 Secondary Flow Generation Models

SECTION 2.0
ANALYTICAL APPROACH

A. Overview

The forced mixer consists of a convoluted lobe section and a mixing chamber. Observations have proven that the lobe region is responsible for the secondary flow generation while the downstream duct region to the nozzle exit plane produces the resultant flow mixing. It is reasonable therefore to propose zonal analytical approach, wherein regions are treated using locally applicable techniques. The convoluted lobes can be viewed as a ring wing with a periodic "spanwise" loading distribution, $\Gamma(\theta)$, as is shown in Figure 5. The periodic lobe cambering produces a nonuniform loading distribution and a corresponding shed vorticity field where strength varies periodically in θ. The shed vorticity is associated with crossflow velocity field (secondary flow) that "mixes" the flow as it is convected downstream. The vorticity is then stretched and eventually dissipated in the mixing chamber through the action of viscosity.

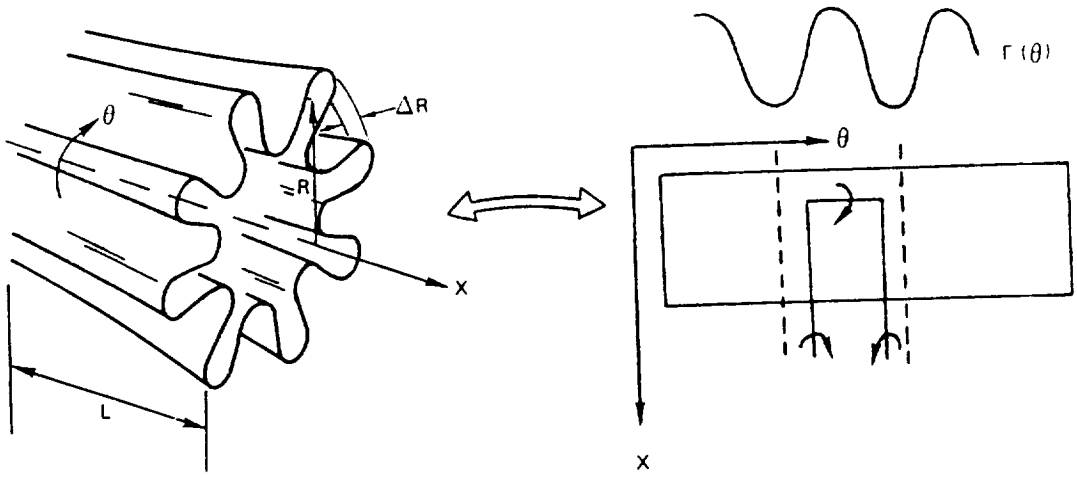

Figure 5 - Ring Wing Analogue of Forced Mixer

A complete inviscid treatment of the three-dimensional lobe region is still a difficult problem, due to geometrical complexity, multiple energy streams and compressibility. Considering the lack of certainty about the relevant driving mechanism for the secondary flow generation, it is appropriate to consider a more approximate analysis that can verify the magnitude of the flap vorticity model. By neglecting the effect of wall boundary layer development, the flow can be considered as irrotational regions separated by a vortex sheet. Downstream of the lobe structure, the flows can initially considered to be inviscid also, with the wake modeling all of the energy jump. An analysis in terms of a velocity potential, defined within each region, is therefore possible.

The mixer lobe surface is characterized by two length scale ratios, which provide relative measures for the lobe height, axial and azimuthal variations.

$$\varepsilon_1 = \frac{\Delta R}{L} \qquad \varepsilon_2 = \frac{N\Delta R}{2\pi R}$$

where N is the number of lobes, L the axial length and Δ R the lobe height above some mean reference radius. For many current designs, the lobes are axially slender ($\varepsilon_1 \ll 1$) and the local Mach numbers are low enough that a small disturbance model may be introduced as a means for treating the salient features of the lobe mixer problem. In the next section a unique small disturbance formulation will be developed that will analytically uncouple the θ variation and reduce the problem to the solution of a sequence of axisymmetric problems. These problems can be solved by taking advantage of previous experience [8] whereby the effects of power addition and "exact" surface boundary conditions were modeled. In contrast to this earlier work, a finite volume cylindrical grid formulation similar to that of Wedan and South's [9] is used. This approach yields a straightforward treatment of extremely general geometries. Although Wedan's calculations have been applied to essentially symmetric geometries, the method presented below will have no such restrictions.

The power contribution and lobe loading result in a potential jump $[\phi]$ across the wake shed from the lobe trailing edge. The corresponding induced secondary flow has a net circulation Γ. By appropriately choosing the closed path of integration over half a lobe, as shown on Figure 6, the circulation integral reduces to

$$\Gamma = [\phi]_{\theta=0} - [\phi]_{\theta=\theta_0} \qquad (1)$$

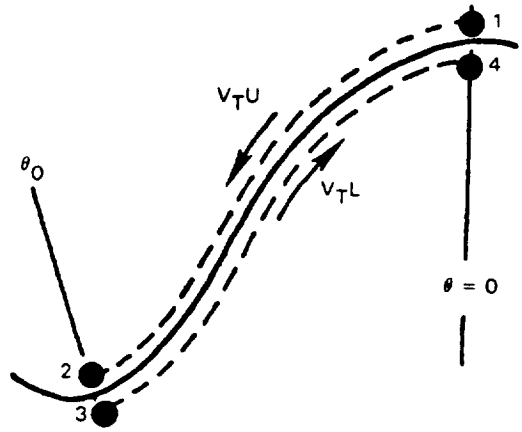

Figure 6 - Schematic of Lobe Trailing Edge Integration Path

In the following sections, a potential analysis for the forced mixer will be developed. The complex three-dimensional problem previously described will be linearized permitting an uncoupling of its θ dependence in the governing equations. Special treatment of surface and Kutta conditions however will be needed to insure compatibility with the governing equations and the physics of the problem, while also uncoupling their θ dependence. Finally the treatment of power addition within a potential format will be developed.

B. Potential Flow Analysis

The inviscid lobe analysis will be applied to the flow domain between the fan and core flow discharge plane and a downstream plane in the mixing chamber, schematically shown on Figure 6. The plane should be displaced sufficiently from the nozzle exit plane so as to avoid nonlinear compressibility effects.

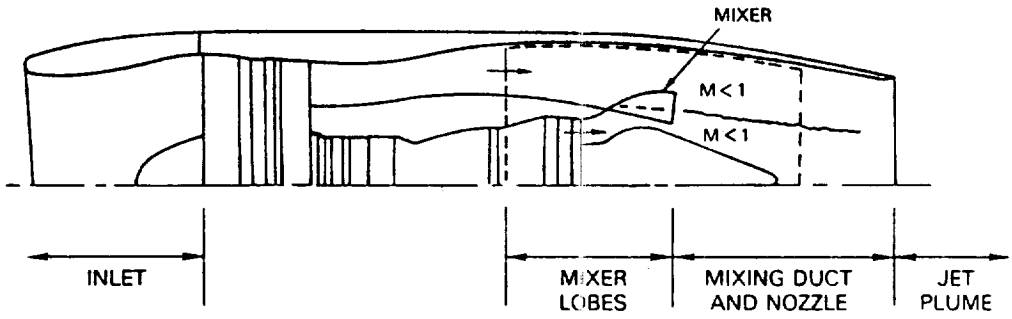

Figure 7 Mixed Flow Nacelle Analysis Domain

The governing equation of mass conservation, applied to an arbitrary control volume in space, yields

$$\oint \rho \vec{v} \cdot \vec{n}\, dA = 0 \tag{2}$$

The nondimensionalized mass flux is defined in terms of a perturbation flow from an upstream subsonic x-"aligned" flow as follows

$$\rho \vec{v} = 1 + \beta^2 \phi_x \vec{i}_x + \phi_r \vec{i}_r + \frac{1}{r} \phi_\theta \vec{i}_\theta \tag{3}$$

where $\beta^2 = 1 - M^2_\infty$ and ϕ is the perturbation potential. Only the linear terms have been retained in Equation (3). The expansion is made assuming that all surfaces can be considered to have slender shapes in the streamwise direction.

Separation of Variables and Numerical Approach

Appropriate surface boundary conditions can be derived from a flow tangency condition given by:

$$\vec{v} \cdot \nabla F = 0 \tag{4}$$

where $\vec{v}$, the velocity vector is given in terms of a velocity potential and F is a general surface described in terms of the r, ϕ, x cylindrical coordinate system

$$F(r, x, \theta) = r - f(x,\theta) = 0 \tag{5}$$

If the velocity potential is assumed to be a perturbation about the upstream axial flow and if the perturbation velocity components are assumed small relative to the upstream flow, then the axial perturbation potential contribution can be neglected and the surface boundary condition reduces to an expression for the surface radial velocity on a mean surface $R_m(x)$.

$$\phi_r = f_x + \frac{f_\theta}{R_m^2} \phi_\theta \tag{6}$$

The perturbation or small disturbance approximation is equivalent to limiting surface slopes to order ϵ_1. This linearization of the boundary condition is needed to render the overall problem separable, as will be seen shortly. At first glance, it appears that the last term in Eq. (6) is of order ϵ_1, however, no such perturbation restrictions has been imposed in the azimuthal direction. The terms, f_x, f_θ are known functions which describe the lobe geometry.

Problem closure is obtained by imposing a quasi one-dimensional analysis for definition of the inlet flux and a Kutta condition to uniquely set the net circulation. In order to simplify the analysis, a cylindrical coordinate system orientation was used to simplify evaluation of the flux integral (2).

Normally, a body conforming or sheared Cartesian grid would appear the logical choice for a coordinate mesh. By treating the mixer with a pure Cartesian grid, the following analysis will be more tractable. Furthermore, one can also substitute storage of large arrays with the additional complexity of irregular boundary/mesh intersections. Analysis of complex geometries in two- and three-dimensions can be easily treated using such a scheme. The mixer lobe geometry is assumed to have no scalloping and scarfing so that the trailing edge will align with the mesh. Extensions of the analysis to include scarf effects will be discussed in an Appendix. Consider the situation where the general three-dimensional lobed mixer problem is perturbed about some mean surface. It is possible to avoid analyzing the full three-dimensional problem be recognizing that the flow is a periodic function of the number of lobes. Solutions to Equation (2) and any appropriate boundary conditions are therefore assumed to be separable, i. e.,

$$\phi\,(x,r,\theta) = g(x,r)\,h(\theta) \tag{7}$$

Combining Equations (2,3,7), the governing flux balance equation terms can be appropriately separated into terms that are either a function of (r,x) or of θ alone,

$$\frac{\text{E-W}\int\beta^2 g_x r\,dr + \underset{\text{N-S}}{\int} r g_r\,dr}{\underset{\Delta A}{\int} g\,\frac{dr}{r}\,d\,x} = -\frac{-h_\theta}{\int h\,d\theta} = K^2 \tag{8}$$

where K is the separation constant and the E-W, N-S and ΔA integrals are elemental areas evaluated in the (x,r) plane. The θ component of Equation (8) can be recast to identify the periodic nature of the separated variable. The solution for h(θ) includes linear combinations of trigonometric functions, where appropriate application of a symmetry boundary condition at the lobe crest simplifies this to

$$h_k = B_k \cos\left(k\,\frac{\pi}{\theta_0}\,\theta\right) \qquad k = 0,1,2,\ldots NH \tag{9}$$

where $K = k\theta/\theta_0$, θ_0 is the half angle of the lobe (crest to trough), NH is the number of harmonics used in the Fourier series, and B_k is a sequence of unknown coefficients still to be determined. The k = 0 solution corresponds to the axisymmetric solution limit. Since the separation constant can take on multiple values, the potential assumes a more general form

$$\phi = \sum_k g_k h_k$$

The axisymmetric component of Equation (8) can be evaluated for an arbitrary point in the flow field on integrals aligned to the cylindrical mesh (Figure 8a) to produce

$$\underset{E-W}{\int} \beta^2 g_{x_k}\, r\,dr + \underset{N-S}{\int} g_{r_k}\, r\,dx - K^2 \int_{\Delta A} \frac{1}{r}\, g_k\, dr\,dx = 0 \qquad (10)$$

The last integral is a source term integrated over the enclosed area ($dr\,dx$). Evaluating the flux balance Equation (10) on an arbitrary flow element yields

$$- \left(\beta^2 g_{x_k}\right)_W A_W + \left(\beta^2 g_{x_k}\right)_E A_E + \left(g_{r_k}\right)_N A_N - \left(g_{r_k}\right)_S A_S - g_k \frac{K^2}{\bar{r}_c} \Delta\bar{A} = 0 \qquad (11)$$

$$k = 0, 1, 2, \ldots NH$$

where the r term has been approximated by its value of the center of each flux cell.

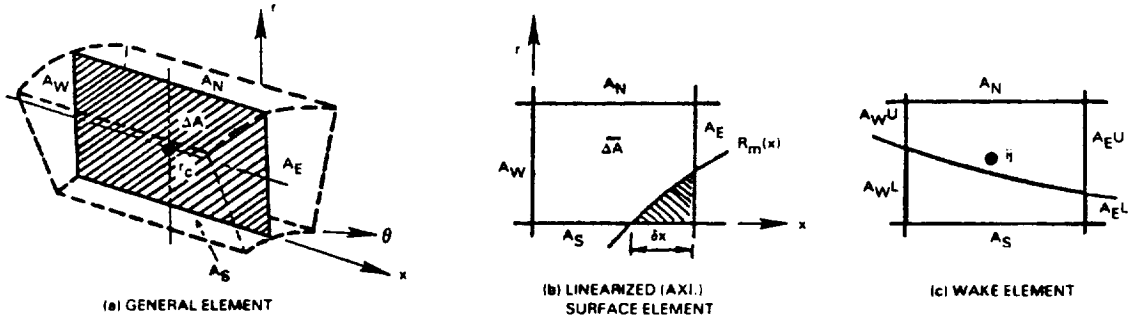

Figure 8 - Cartesian Flux Volume Element Description

Equation (11) is a discrete approximation whose subscripts refer to the respective faces of the elemental volume shown on Figure 8a. Central differencing of the flux terms and collecting the contributions at each node results in a tridiagonal equation system in terms of g_{ijk}.

$$A_j\, g_{i,j-1,k} + B_j\, g_{i,j,k} + C_j\, g_{i,j+1,k} = W_{j,k} \qquad (12a)$$

$$k = 0,1,2,\ldots NH$$

where

$$A_j = \frac{A_S}{\Delta r} \qquad (12b)$$

$$B_j = -\left[\frac{\beta^2}{\Delta x}\left(A_E + A_W\right) + \frac{1}{\Delta r}\left(A_N + A_S\right)\right] - K^2\frac{\Delta A}{r_{ij}} \qquad (12c)$$

$$C_j = \frac{A_N}{\Delta r} \qquad (12d)$$

$$W_{j,k} = -\frac{A_W}{\Delta x}\beta^2\, g_{i-1,j,k} - \frac{A_E}{\Delta x}\beta^2\, g_{i+1,j,k} \qquad (12e)$$

Closure to the problem formulation requires application of boundary conditions on the boundaries of the domain of integration. Referring to the computational outline in Figure 7, the no flow condition will be imposed on all solid surfaces. The upstream flows normally are defined in terms of the engine discharge conditions, but flow continuity (Kutta condition) at the lobe trailing edge necessitates an alternate approach to avoid overspecifying the inlet conditions. These boundary conditions will be explained in the following sections.

Surface No-Flow Boundary Condition

In a flux formulation, the no-flow boundary condition is implemented as a zero flux condition on all solid surfaces. The flux balance for an element intersecting the three-dimensional lobe surface is not separable along the lines previously derived. In order to render the problem separable, the boundary conditions must be linearized in the θ direction resulting in a modified boundary condition with a source-like term applied on a mean axisymmetric surface, $R_m(x)$. The surface intersecting computational element effectively looks like Figure 8b. The flux balance on such an element must be modified by an additional source term representing the "surface" flux ($\bar{g}_r$) in the r direction,

$$\int_{E-W}\beta^2\, g_{x_r}\, r\,dr + \int_{N-S} g_{r_k}\, r\,dx - \int_{Rm}\bar{g}_{r_k}\, r\,dx - K^2\int_{\overline{\Delta A}} g_k\,\frac{dr\,dx}{\bar{r}} = 0 \qquad (13)$$

$$k = 1,2,\ldots NH$$

The areas in the integrals describe only the external portion of the cell on the side and azimuthal ($\%\bar{A}$) faces.

By applying the mean radius approximation to the contour, one can also express the lobe surface in terms of separable variables, i. e.,

$$f(x,\theta) = R_m(x) + \sum_{k=1}^{NH} \lambda_k(x)\, h_k(\theta) = \sum_{k=0}^{NK} \lambda_k(x)\, h_k(\theta) \qquad (14)$$

where $\lambda_0(x)$ is the axisymmetric modal shape and may be used as a mean radius. A Fourier moment analysis couples the θ dependence of the contour with dependent variables. The unknown coefficients λ_k are determined by using the angular definition shown on Figure 9 and arbitrarily defining the potential within a constant B_k.

$$\lambda_k(x) = \frac{1}{\theta_0}\int_{-\theta_0}^{\theta_0} f(x,\theta)\, \cos\left(\frac{k\pi\theta}{\theta_0}\right) d\theta$$

$B_k = 1$

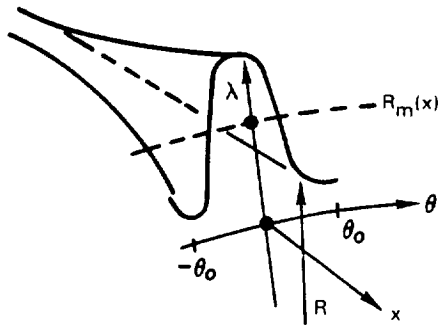

Figure 9 - Domain Definitions for Moment Analysis

Substituting the modal description of the geometry into the no-flow condition and taking advantage again of the orthogonality of alternate Fourier modes for the g_k's on the boundary, reduces the surface boundary condition to a flux along a mean surface, which is given by

$$\bar{g}_{r_k}(x, R_m) = \lambda_k(x) + \frac{1}{2R_m^2} \sum_j \sum_n \lambda_n(x)\, g_j(x,R_m) \left[\delta_{k,n-j} - \delta_{k,n+j}\right] \qquad (15)$$

$$k = 0,1.2,\ldots NH$$

where δ_{ij} is the Kronecker delta function. The first term on the right side is the primary contribution to a given mode. The second term represents a coupling of the different modal solutions due to the product $f_\theta \phi_\theta$ in the no-flow equation. If parameter ε_2 is small, this term is absent. Observe that Equation (15) is a mixed type boundary condition. Therefore, the solution algorithm cannot explicitly determine the $g_k(x,r)$'s from the given boundary conditions. This problem of coupled modal equations is alleviated by lagging the alternate modes in the iterative solution that will be discussed shortly.

The modal solutions for the functions $g_k(x,r)$ can be discriticized along to the cylindrical mesh to yield

$$-\beta^2 g_{x_{kw}} A_w + \beta^2 g_{x_{kE}} A_E + g_{r_{kN}} A_N - g_{r_{ks}} A_s - \overline{g}_{r_k} \overline{R}_m \delta x - \frac{K^2}{R_m} g_k \overline{\Delta A} = 0 \qquad (16)$$

$$k = 0,1,2,\ldots NH$$

where A denotes the exterior portions of the areas of the intersected cells and $\Delta\overline{A}$ the exterior area of its azimuthal face, see Figure 8b. In general, a surface element includes a region of flow and a region interior to the body. Along the mean surface however, an element includes a core flow and fan flow region. Correct flux balancing in each region is expedited by tracking the potentials of each flow separately across the surface.

Discriticizing the boundary Equations (15) and (16) is complicated by the mixed mode term in the "surface" flux. In order to solve the equations numerically, the coupled term is introduced into the $W_{j,k}$ right side term and lagged in the iterative solver, i. e.,

$$W_{j,k} = W_{j,k} + \overline{R}_m \delta x \left(\lambda_k + \frac{G_2}{2R_m^2} \right) \qquad (17a)$$

$$B_j = B_j + \overline{R}_m \frac{\delta x}{2R_m^2} G_1 \qquad (17b)$$

where G_1 and G_2 are the coefficients from Equation (15) of the kth mode and the mixed modes (minus the kth term) respectively.

Solution Algorithm

The governing equations and boundary conditions reduce the analysis problem to a system of linear algebraic equations in terms of the $g_k(x,r)$'s and correspondingly the velocity potential. These equations are solved iteratively using a successive line over-relaxation procedure (SLOR). To optimize the calculations, a grid halving algorithm is utilized. In such an algorithm, the previous coarse grid solution is interpolated onto the next or finer grid as its initial guess. The solution convergence on each grid is monitored by

tracking either the residual, defined as the normalized error in the mass conservation equation at the nth iterate, or the jump in potential at the splitter trailing edge. This latter variable is the "flap" vorticity discussed in the introductory remarks. Typically the residual is a monotonically decreasing function that, in a SLOR scheme, achieves only a two orders of magnitude reduction per grid. Finally, the results are displayed in terms of the pressure coefficient defined for each stream relative to its own upstream dynamic head.

Inlet Flow Boundary Conditions (Compound Choked Flow Analysis)

Flow requirements for cruise engine operating conditions are typically determined by engine power settings as well as by inlet and nozzle exit areas. Analysis of the localized mixer/nozzle problem requires a completely specified set of boundary conditions; however, precautions must be taken to avoid specifying inconsistent fan and engine core flow conditions such that the Kutta condition at the lobe trailing edge will not be maintained. For example, if the onset flows each were specified in terms of p_0, T_0 and M, the problem could be over-defined. Use could be made of the nozzle exit flow conditions in conjunction with the wake contact surface matching conditions to determine uniquely the fan and core flow requirements. The problem is further complicated by trying to insure that the analysis would include both choked and unchoked conditions at the nozzle exit plane. Table I details duct operating conditions for several mixed flow installations. The table indicates that the nozzle exit operating condition is dependent on the mission profile of the aircraft and that choked and unchoked conditions are indeed possible.

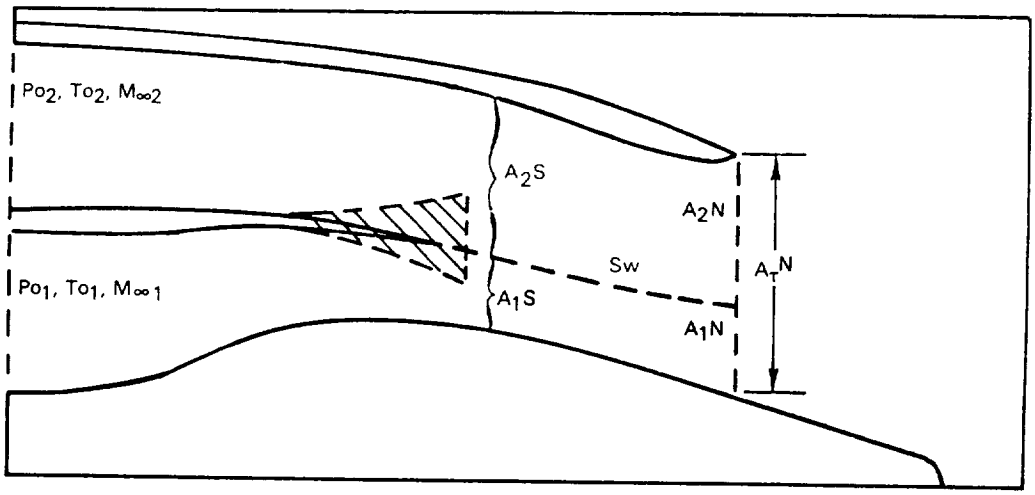

Figure 10 Dual Stream Choked Flow Domains

TABLE I
TYPICAL MIXER DUCT OPERATING CONDITIONS
(Standard Day)

		E^3	JT8D-209 (Super 90)		JT15D (no scallop)
		SLTO	SLTO	Avg. Cruise	SLTO
	Tamb	543.7	519.0	393.8	519.0
	Pamb	14.7	14.7	3.46	14.7
Fan	T_{OF}	625.6	627.5	560.2	602.5
	P_{OF}	22.45	24.36	9.33	22.04
	W_F	1157.2	299.1	120.1	55.5
Primary	T_{OP}	1490.0	1276.0	1221.0	1534.0
	P_{OP}	21.65	25.60	10.1	21.09
	W_p	159.6	161.4	70.5	21.1
	AF	36.01	1080.0	1080.0	173.06
	Ap	908.0	648.3	648.3	130.9
	A_N	--	1096.7	1096.7	304.0
Nozzle	T_{ON}	737.3	864.1	814.3	919.4
	P_{ON}	22.20	24.76	9.60	21.46
	ΔMIX	85.0Δ	92.0Δ	92.0Δ	84.0Δ
	P_{ON}/P_{oo}	1.50	1.68	2.78	1.46
	Condition	Unchoked	Unchoked	Choked	Unchoked

The analysis developed is based on a compound nozzle model, wherein the curvature induced traverse pressure gradients are neglected and the static pressure is only a function of axial position. Approximating the nozzle exit flow by a quasi-one dimensional flow, the continuity equation for a single flow

$$d\,(\rho v A(x)) = 0 \tag{18}$$

and the isentropic forms of the energy equation can be combined to give

$$\frac{dA}{dx} = \frac{A}{\gamma}\left(\frac{1}{M^2} - 1\right)\frac{d}{dx}\ln p \tag{19}$$

This equation has been generalized [11] for multistream flows as follows

$$\frac{dA_i}{dx} = \frac{A_i}{\gamma_i}\left(\frac{1}{M_i^2} - 1\right)\frac{d}{dx}\ln p \tag{20}$$

where quasi-one dimensional matching conditions across each dividing streamline prevent mixing but allow pressure communication (p_i=p) across the flow. But area continuity

$$A_T = \sum_i A_i$$

therefore,

$$\frac{dA_T}{dx} = \sum_i \frac{dA_i}{dx} = \nu \frac{d}{dx}\ln p$$

where ν , the compound flow indicator is

$$\nu = \sum_i \frac{Ai}{\delta_i}\left(\frac{1}{M_i^2} - 1\right) \tag{21}$$

Reference [10] also demonstrated that the nozzle flow exit state corresponds to the sign of ν, i.e.,

$\nu > 0$ compound subsonic
$\nu = 0$ compound sonic
$\nu < 0$ compound supersonic

Equation (21), in conjunction with the definition of the local mass flows, in terms of their stagnation properties,

$$w_i = w_i\,(A_i, p_i, p_{o_i}, T_{o_i}) \tag{22}$$

and the isentropic relation are sufficient to provide closure of the problem. For a dual stream flow, equation (21) becomes

$$\nu = \frac{A_1^n}{\gamma_1} \frac{1}{M_{1n}^2} - 1 + \frac{A_2^n}{\gamma_2} \frac{1}{M_{2n}^2} - 1 \tag{23}$$

The superscripts refer to axial locations defined on Figure 10. This can be further reduced using equation (40). In particular, assume that the flow at the nozzle plane is subsonic, then

$$P_2^n = P_1^n = P_\infty$$

and the compound flow parameter becomes

$$\nu = \frac{A_1^n}{\gamma_1}\left[\frac{1}{\left(\frac{2}{\gamma-1}\right)\left[\left(\frac{P_{01}}{P_\infty}\right)^{\frac{\gamma_1-1}{\gamma_1}} - 1\right]} - 1\right] + \frac{A_2^n}{\gamma_2}\left[\frac{1}{\left(\frac{2}{\gamma_2-1}\right)\left[\left(\frac{P_{02}}{P_\infty}\right)^{\frac{\gamma_2-1}{\gamma_2}} - 1\right]} - 1\right] \tag{24}$$

The value of ν is not determinate in its present form, since A_1 , A_2 are not known. An iteration to determine these areas follows.

(a) Guess value for p_1^m for given P_{01}, A_1^n, A_1^m, A_2^m.

(b) Calculate w_2 from following equation given in Reference 11.

$$w_2 = [w_1] \left[F\left(T_{01}, T_{02}, A_1, A^*, P_{01}, P_{02}, P_\infty\right)\right] \tag{25}$$

(c) Determine the new value of $\overline{P}_1^m$ from equation (22)

$$w_2 = w_2 \left(A_2^m, \overline{P}_1^m, P_{02}, T_{02}\right)$$

but under relax update according to the following

$$p_1^m = \overline{p}_1^m + \alpha \left(p_1^m - \overline{p}_1^m\right)$$

and continue iteration until ΔP_1^m within given tolerance.

(d) Determine

$$w_1 = w_1 \left(A_1^m, p_m^m, P_{01}, T_{01}\right)$$

(e) Determine A_1, A_2 using equation (22), i.e., solve

$$w_1 = w_1 \quad (A_1^n, p_\infty, p_{0_1}, T_{0_1}) \quad \text{for } A_1^n$$

(f) Calculate ν according to equation (21).

If $\nu<0$, then the solution is complete and the flows are defined in terms of the given upstreams data and the flows determined in iteration (a-f). If $\nu=0$, then the flow is compound choked and p_e is not p_∞.

For compound choked flow, a dual iteration is performed to find the exit pressure for a convergent nozzle, and the splitter exit plane static pressure. In this case, it is known that the compound flow indicator $\nu = 0$. An initial guess for the primary and secondary nozzle flow areas is given by:

$$A_1^n = A_t^n \quad (A_1^s/A_t^s)$$

$$A_2^n = A_t^n \quad (A_2^s/A_t^s)$$

Using equation (24) with p_∞ replaced by p_e, an iteration is performed until a value of p_e is obtained which gives $\nu = 0$. Now the primary and secondary flows can be computed from the continuity equation (22) at the exit. The secondary flow continuity equation is then used to compute the splitter exit pressure, which is then used to compute a primary splitter exit flow. If this flow does not match the primary nozzle flow, a new primary and secondary nozzle area are computed using the primary splitter exit flow, and the entire choked flow calculation is repeated until the flows balance and $\nu = 0$.

Finally, with the flows, pressures and temperatures in both streams known, the reference Mach numbers at the inlet plane for each stream are computed from the continuity equation (22) and the isentropic equations. The velocity gx of each stream is therefore directly known. In the present analysis, it is assumed that $gx = g_{x0}$ while all higher nodal derivatives at the inlet plane are identically zero.

Kutta condition - Powered Wake Analysis

Treatment of the flow downstream of an arbitrary body is complicated by the unique interaction of the stream from above and below the body. Even in nonpowered situations, the lift of flow turning is reflected as a jump in potential convected from the sharp trailing edge. This jump will remain constant and will follow the trailing stagnation streamline. In the situation of power addition, streams are assumed locally irrotational with different energy levels. They inviscidly interact through the local potential jump that is determined from the basic consistency conditions across a "contact discontinuity," i.e., static pressure match on the wake or vortex sheet Sw and streamline slope continuity

$$\vec{v} \cdot \vec{n} = 0 \quad \text{on } S_w, S_w$$

Classical linear theory assumes the wake lies along a constant radius surface (Rm) from the trailing edge, and the streamline slope condition is relaxed. Flow is permitted to cross through the constant radius. Consistent with the surface boundary condition formulation, the wake can be modelled by a mean or axisymmetric surface that varies with axial position.

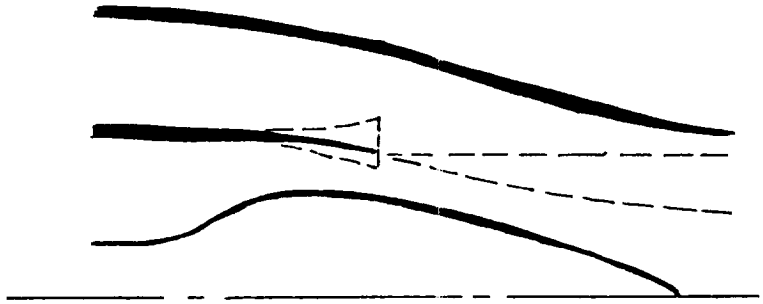

Consider the mass flux balance on an element that includes an arbitrarily oriented mean wake streamline (Figure 8c). Applying the flux balance (16) to the upper and lower portions of the (ij) element results in equations that assume a mass flux can exist across the given wake contour, thereby allowing a lagging of the wake path in the iteration cycle. Adding the conservation components together will produce an equation for the ij^{th} element where the flux contributions across the wake $\overline{g}_r^{\,u,L}$ identically cancel each other out. If the potentials on both sides of the wake are defined in terms of a mean potential and a wake jump $[g_k]$ as follows

$$\overline{g}_{ijk} = \frac{1}{2} \left(g^u_{ijk} + g^L_{ijk}\right) \tag{26a}$$

$$[g_k]_{ij} = \left(g^u_{ijk} - g^L_{ijk}\right) \tag{26b}$$

the flux balance for a wake element becomes

$$A^L_j \,\overline{g}_{i,j-1,k} + \left(B^u_j + B^L_j\right) \overline{g}_{i,j,k} + C^u_j \, g_{ij+i,k} = W^u_{j,k} + W^L_{j,k} - \frac{[g_k]_{ij}}{2} \left(B^u_j - B^L_j\right) \tag{26c}$$

$$k = 0,1,2,\ldots\ NH$$

This Equation corresponds to one row in the general (JMxJM) tridiagonal matrix for the i_{th} line,

$$\left|\begin{array}{ccccccc} \ddots & \ddots & \ddots & & & & \\ A_{j-1} & B_{j-1} & C_{j-1} & & & & \\ & A^L_j & \left(B^L_j + B^u_j\right) & C^u_j & & & \\ & & A_j & B_j & C_j & & \\ & & & \ddots & \ddots & \ddots & \end{array}\right| \tag{27a}$$

The structure of the matrix is equivalent to the following (JM+1) x (JM+1) tridiagonal matrix

$$\begin{vmatrix} \ddots & \ddots & \ddots & & & \\ A_{j-1} & B_{j-1} & C_{j-1} & & & \\ & A_j^L & B_j^L & o & & \\ & & o & B_j^u & C_j^u & \\ & & & A_{j+1} & B_{j+1} & C_{j+1} \end{vmatrix} \qquad (27b)$$

The two new (ij^{th}) equations are similar to individual wake element flux balances with the added proviso that the A terms are zero. This is equivalent to assuming that the wake is a solid boundary since all boundary areas are assumed by the program logic to be zero. Under such a format, the program can automatically treat these constructed equations in the algorithm and the real wake equation is arrived at by contracting or adding the appropriate equations.

The matrix solution for the i^{th} row needs an algorithm for defining the $[g_k]$ and for updating the wake path. The potential jump, $[g_k]$ is obtained from the constraints of static pressure and streamline slope continuity. Expressing the flows relative to the same reference freestream static pressure, the pressure match condition reduces to

$$C_{pu} = \frac{\gamma_L M_\infty^2}{\gamma_u M_u^2} C_{p_L} + \frac{2 \Delta P_\infty}{\gamma_u M_{\infty_u}^2} \qquad (28)$$

The pressure coefficient Cp can be taken from the general isentropic definition or from a formulation consistent with our linearized algorithm and thus separate out the axisymmetric component on each mode $\bar{C}_{p_k}$.

$$\bar{C}_{p_k}(x,r) = -2\, g_{x_k}(x,r) \qquad (29)$$

The streamline slope matching conditions, along the general wake contour

$$\frac{\phi_r^u}{1 + \beta_u^2 \phi_x^u} = \frac{\phi_r^L}{1 + \beta_2^2 \phi_x^L} \qquad (30)$$

can also be simplified by assuming that the axial velocity flux contribution is small relative to unity, then

$$\phi_r^u = \phi_r^L \qquad \text{or for each mode} \qquad g_{r_k}^u = g_{r_k}^L$$

If the slope

$$\frac{dr}{dx} \equiv g_{r_k} \equiv o,$$

the wake follows the constant radius approximation.

In order to obtain closure (Kutta condition) for the problem an additional assumption is needed. Although the global Kutta condition,

$$C_{pu} = C_{pL} \tag{31a}$$

needs to be maintained individual modes need their own boundary condition. It is proposed therefore that each mode satisfy

$$g^u_{x_k} = g^L_{x_k} \tag{31b}$$

and therefore equation (31) is implicitly satisfied. Equations (28b), (26a,b) are then combined to determine the potential jump

$$[g_k]_x = E_1 \delta_{ok} + E_2 \bar{g}_{x_k} \tag{32}$$

Ideally, the jump in potential along the wake is obtained by integrating out axially from the trailing edge along the mean radius as follows

$$[g_k]_{ij} = E_1 \delta_{ok} (x-x_{te}) + E_2 \bar{g}_{ki} + \left\{[g_k] - E_2 \bar{g}_k\right\}_{TE} \tag{33}$$

In the entire preceding discussion, the slope was assumed given. In actuality, the path is evolved as the program interates. A simple streamline tracing procedure could be used to periodically update the wake path. Another attractive approach would be to drive the slope using the nonconservation over the local flux cell.

Equation (1) can now be re-expressed in terms of the separated variables as follows

$$\Gamma = 4 \sum_{k=1}^{NH/2} (\bar{g}_{2k} \Delta U_\infty - [g_{2k}] \bar{U}_\infty)_{TE} \tag{34}$$

where only the odd modes contribute to the net induced circulation field.

C. Geometry Definition

General lobe contour definition can be a complex problem even if scalloping and scarf angle cutouts are not included. Current commercial designs fall within three general categories: radial sidewalls, parallel sidewalls, circular arc sidewalls with the remaining segments of the lobe defined in terms of tangentially intersecting circular arc segments. Considering the periodic nature of the analysis formulated in the previous section, one must limit the geometry capability to axisymmetric duct wall configurations while the lobe cross-section must be limited to radial sidewall geometries to avoid multiple valued structures. Using this approach, a mixer centerbody and fan cowl can be defined and replicated using the BYU Movie Three-Dimensional hidden line graphics program, to produce Figure 10.

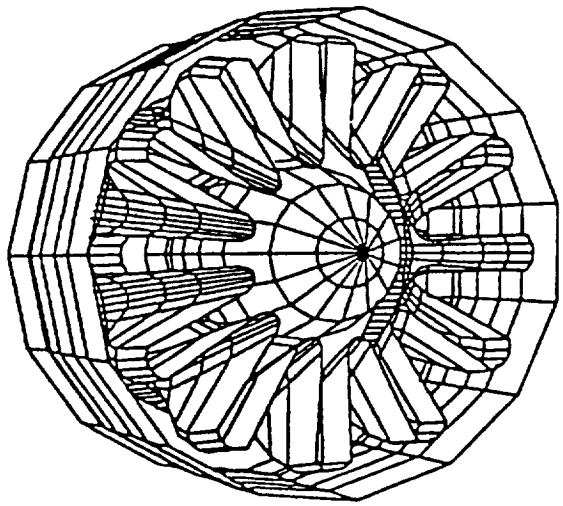

Figure 11 Three Dimensional Display of JT8D-209 Mixer Geometry

A measure of the feasibility of the Fourier decomposition method can be made by considering a finite number of harmonics and comparing the reconstructed lobe versus the given lobe definition. A equal angle series construction permits use of fast Fourier scheme (FFT) to evaluate the Fourier coefficients. The reconstructed lobes are shown in Figure 12 for NH = 1, 3 and 9. The base contour was generated analytically using 50 points. The modal analysis, however, does not demonstrate the perfect agreement. The largest excursions occur at points where the curvature changes instantaneously. Whereas this aspect is commonly found in square wave reconstructions, where a large number of modes must be used to obtain an accurate wave representation, the slight lobe contour mismatch should not be significant in establishing the "flap" vorticity field. The sensitivity of the analysis to the number of modes, however, will be shown below to be a critical factor in determining the mean radius, the leading term obtained from the FFT analysis.

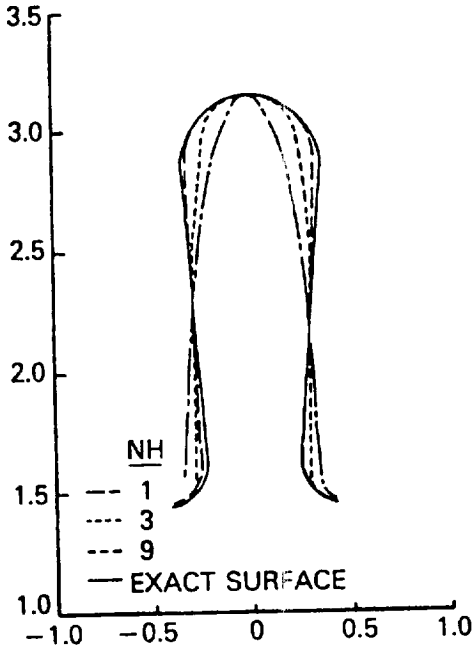

Figure 12 Comparison of Fourier Modal Reconstruction of JT8D Lobe Near Trailing Edge Plane

SECTION 3.0
RESULTS AND DISCUSSION

The analysis (FLOMIX) described in the previous section has been applied to several lobed mixer configuration. When $\lambda_k = 0$ (k=1, 2,...NH), the zeroth mode solution will describe the powered flow over a completely axisymmetric configuration. An initial calculation of a planar mixer lobe in a straight duct is presented to calibrate the analysis. Planar conditions are simulated by considering an axisymmetric geometry at large radius. In such a situation comparison calculations can be made with an available analytically constructed solution that simulates an isolated planar mixer lobe using distributed doublets along a mean planar surface[11] (PLANMIX). Figure 13 shows a sideview of the configuration analyzed. The duct walls are defined sufficiently far from the lobes (H = 8") so that any interactions would be minimal. Numerical calculations demonstrate that there is no potential interaction effect due to these walls. The lobe surface in both calculation methods is generated from a single cosine wave, therefore a single modal (NH = 1) solution models the flowfield. In this study no power addition effects are considered. Predictions are presented for the reconstructed (as a function of θ) components of the perturbation velocity on the lobe surface. Figures 14(a), (b), (c) show comparison calculations between FLOMIX and PLANMIX the three components for several azimuthal cuts running from the lobe crest ($\theta' = 0$) to the inside of the lobe trough ($\theta' = 1.0$). The axial scale runs from the lobe leading edge to its trailing edge. The profiles reflect the effect of the linear theory approximations at the trailing edge, i.e., the Kutta condition is satisfied and the axial velocity perturbation goes to zero. Although both methods are based on linear theories, slight differences should be expected since the planar analysis is an inverse method evaluating singular integrals numerically as input while the present method is a finite difference flux volume scheme.

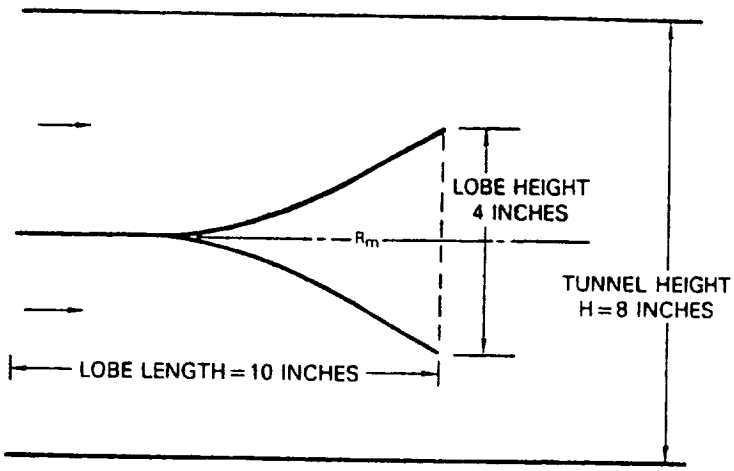

Figure 13 Sideview Representation of Planar Mixer/Wind Tunnel Geometry

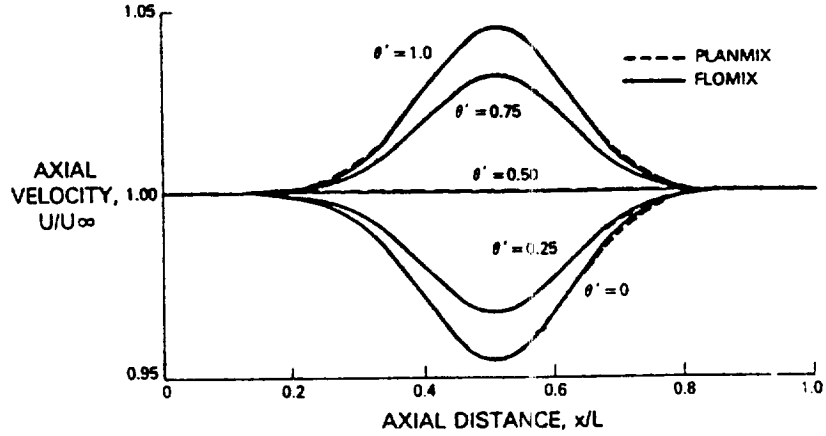

Figure 14a Comparison Calculations of Axial Velocity for a Symmetric Planar Mixer in a Planar Duct

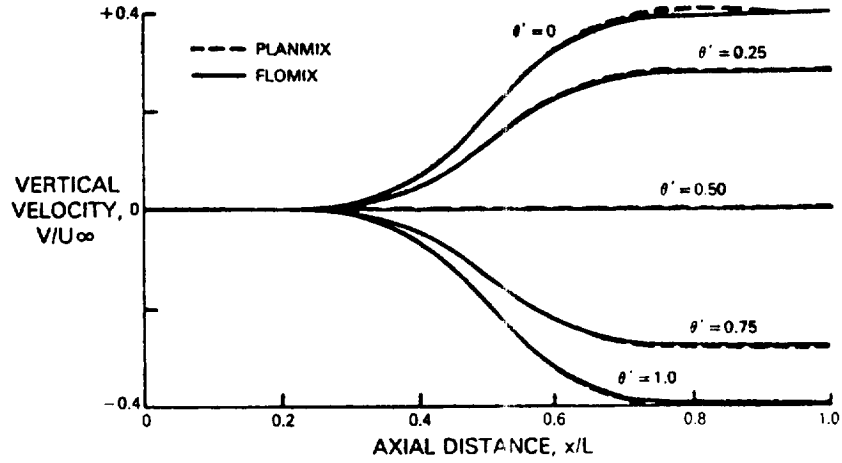

Figure 14b Comparison Calculations of Vertical Velocity for a Symmetric Planar Mixer in a Planar Duct

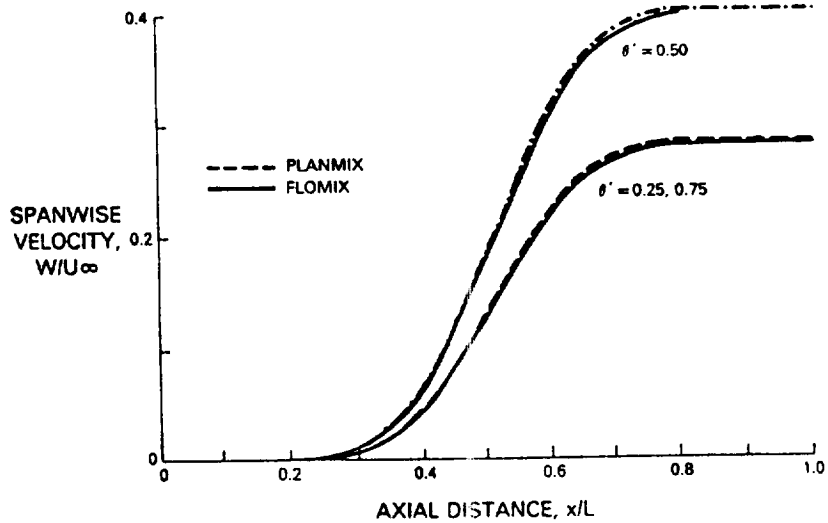

Figure 14c Comparison Calculations of Spanwise Velocity for a Symmetric Planar Mixer in a Planar Duct

More realistic applications of the method can be found by considering flight type configurations. In particular, two specific powered applications are presented due to the "benchmark" nature of their experiments: (1) the Energy Efficient Engine (E^3) configuration 29, which is an 18 lobe forced mixer[12,13], and (2) a JT8D-209 12 lobe forced mixer[5]. The E^3 configuration, shown in Figure 13, is well suited to the present formulation in that although it was modeled for a modern high bypass engine, it was designed specifically for code verification, i.e., no scalloping or scarfing of the lobes was used and extensive surface static pressure surveys were made in the lobe region of the mixer. In contrast, the JT8D-209 forced mixer is a higher penetration 12° scarf angle design typical of first generation low bypass applications. While this geometry is not strictly suitable for code comparison, the experimental data included LDV profile measurements of all components of velocity at the lobe trailing edge. Satisfactory modeling of these lobe cross-sections, even for the JT8D-209 high penetration lobe (Figure 12) is possible with only ten Fourier terms, however, a more definitive approach to defining NH is given below.

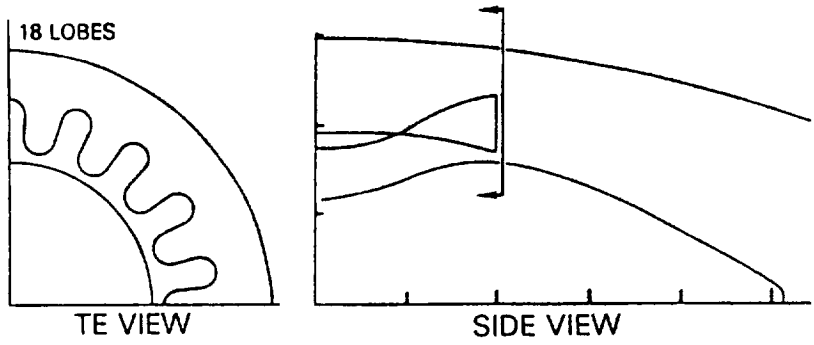

Figure 13 Schentic Representation of E^3 Configuration 29 Lobed Mixer

Postprocessing of the solution produces surface Mach number definition and quantifies the level of "flap" vorticity or circulation through the potential jump at the lobe trailing edge. The surface solutions, although strictly determined along the approximate mean surfaces can be interpreted, to first order, as solutions on the actual surfaces. By examining the potential jump variable, an effort will be made to separately quantify the contributive effects of mean flow turning, power addition and lobe aspect ratio (penetration angle) on the overall mixing process.

Numerical solutions initially have been made for the E^3 configuration 29 lobed mixer and comparisons have been made with test data measured on a full scale model at FluiDyne Engineering Corp. The experimental cruise flow conditions were characterized by power settings* of $\Delta P_o/P_{os} = 0.094$ and $\Delta T_o/T_{os} = 1.50$. Computational simulation of the measured flow conditions is obtained by setting the upstream total conditions in each stream as well as settings the exit static pressure. The quasi one-dimensional choked flow analysis correctly sets up a choked flow at the nozzle exit plane and sets the inlet flows and Mach numbers to within 10% of those measured by the facility flowmeters. Solution accuracy, relative to the level of modal approximation, however, is to be answered.

Table I summarizes the individual modal potential jumps $[g_k]$ obtained from a series of calculations in which different levels of modal approximation (NH = 0,1,2,3...) were used to simulate the E^3 mixer. The calculations were initially made for an axisymmetric configuration where the effect of flow turning of the mean radius (-0.093) and power addition (-0.012) could be identified. With the mean radius having a positive trailing edge angle, these results demonstrate that a positive circulation corresponds to a clockwise rotation. The tabulated calculations varied both the number of harmonic terms (NH) used to represent the θ dependence of the velocity potential and the number of Fourier terms (NF) used to represent the θ dependence of the lobe surface. The tabulated results indicate that while each approximation produces different total and modal potential jumps, the individual modes approach fixed values as more terms are included. Although the higher modal solutions converge much more rapidly than the leading terms, the additional storage required for these higher order terms is impractical. A study of the governing differential equations indicates that the modal coupling is extremely weak for the axisymmetric mode and that its primary driving term is the mean radius, determined from the Fourier analysis. Since higher order solutions (NH large) contribute little to the total circulation field, one can neglect these equations while retaining the addition terms for an improved Fourier (NF) definition. For example, calculations with NH = 3, NF = 5 yield the same modal jumps as NH = 5, NF = 5. In the comparisons described below the solution parameters NH = 5, NF = 18 were used as representative of an "asymptotic" solution.

---

* The subscript s refers to reference conditions in the secondary or fan stream.

TABLE I. POTENTIAL JUMP COMPARISONS [g_k]

NH	NF	Power Addition	Total Jump	k=0	1	2	3	4	5
0	axi (18)	No	-0.093	-0.093					
0	axi (18)	Yes	-0.118	-0.118					
1	1	Yes	-1.396	-1.328	-0.068				
3	3	Yes	-0.527	-0.467	-0.084	0.018	0.006		
5	5	Yes	-0.353	-0.292	-0.087	0.013	0.007	0.006	
3	5	Yes	-0.367	-0.293	-0.087	0.013			
5	9	Yes	-0.263	-0.187	-0.088	0.008	0.009	-0.004	-0.003
Asymptotic Value (NH=5, NF=18)			-0.191	-0.118	-0.089	0.008	0.010	-0.002	-0.003

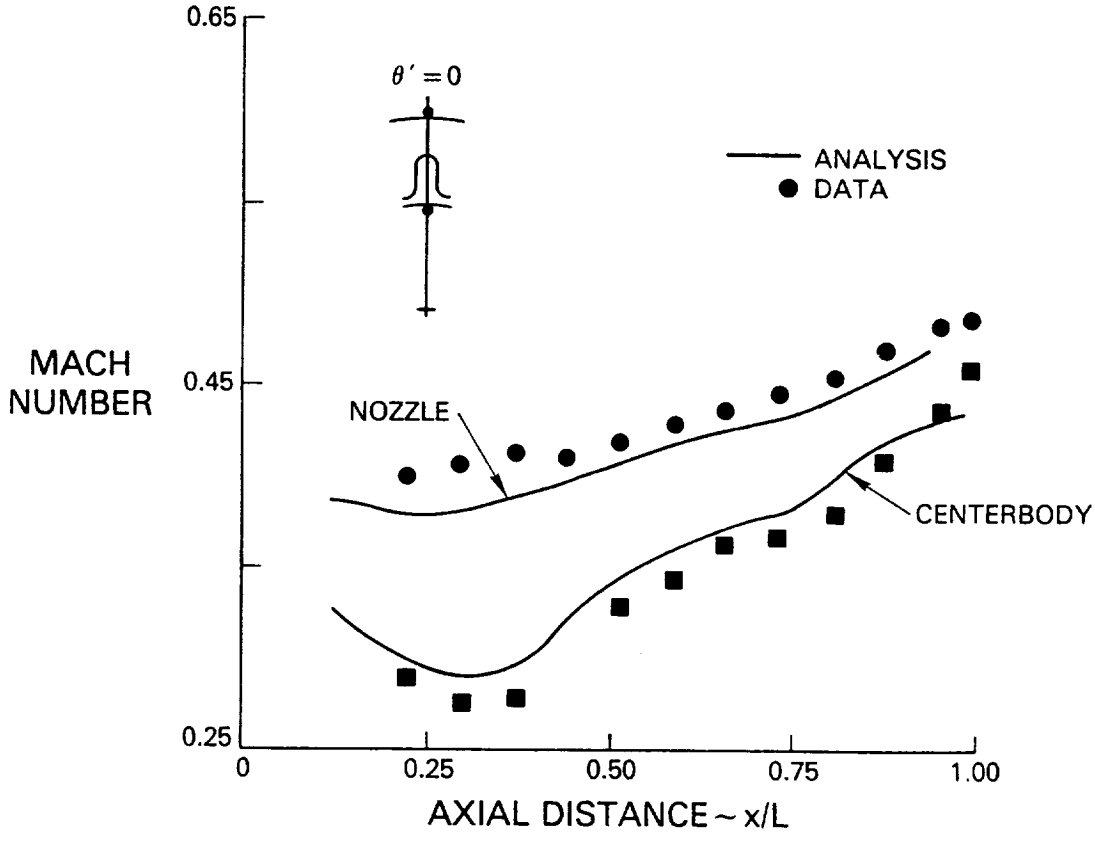

Figure 16 Surface Mach Number Comparisons for E^3 Duct Walls at Lobe Crest Orientation

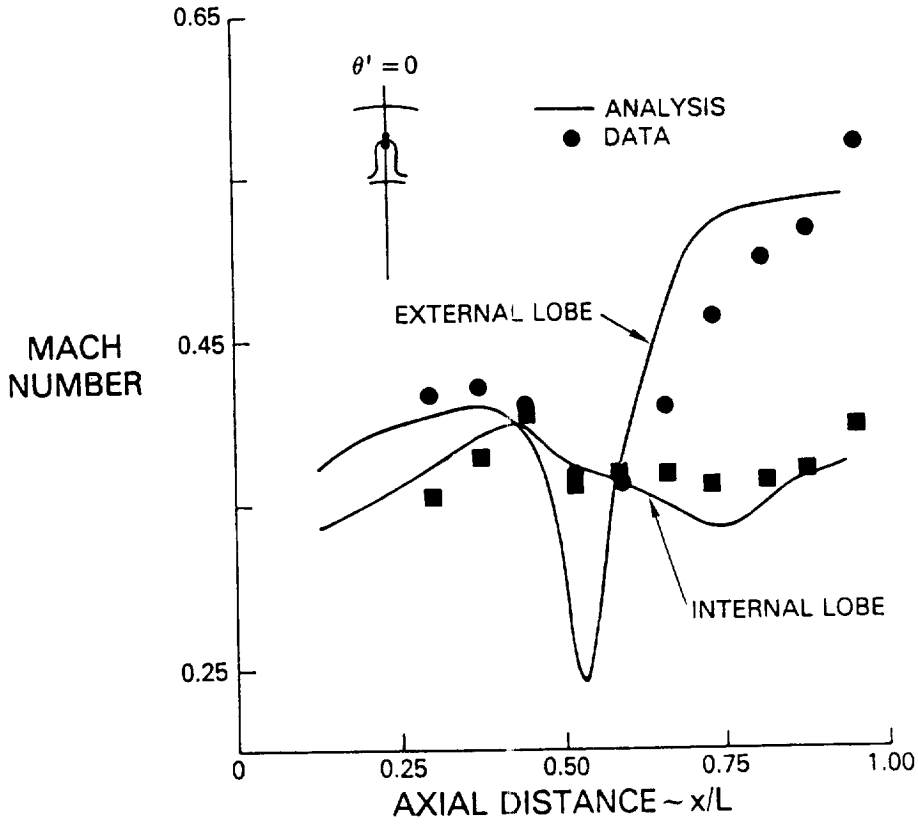

Figure 17 Surface Mach Number Comparisons for E^3 Mixer Lobe at Lobe Crest Orientation

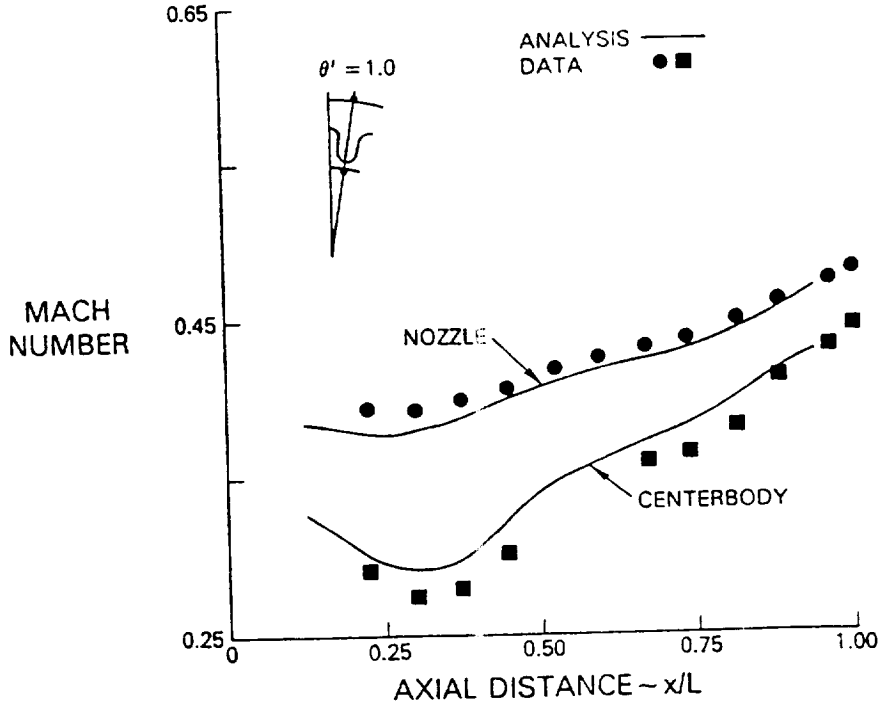

Figure 18 Surface Mach Number Comparisons for E^3 Duct Walls at Lobe Trough Orientations

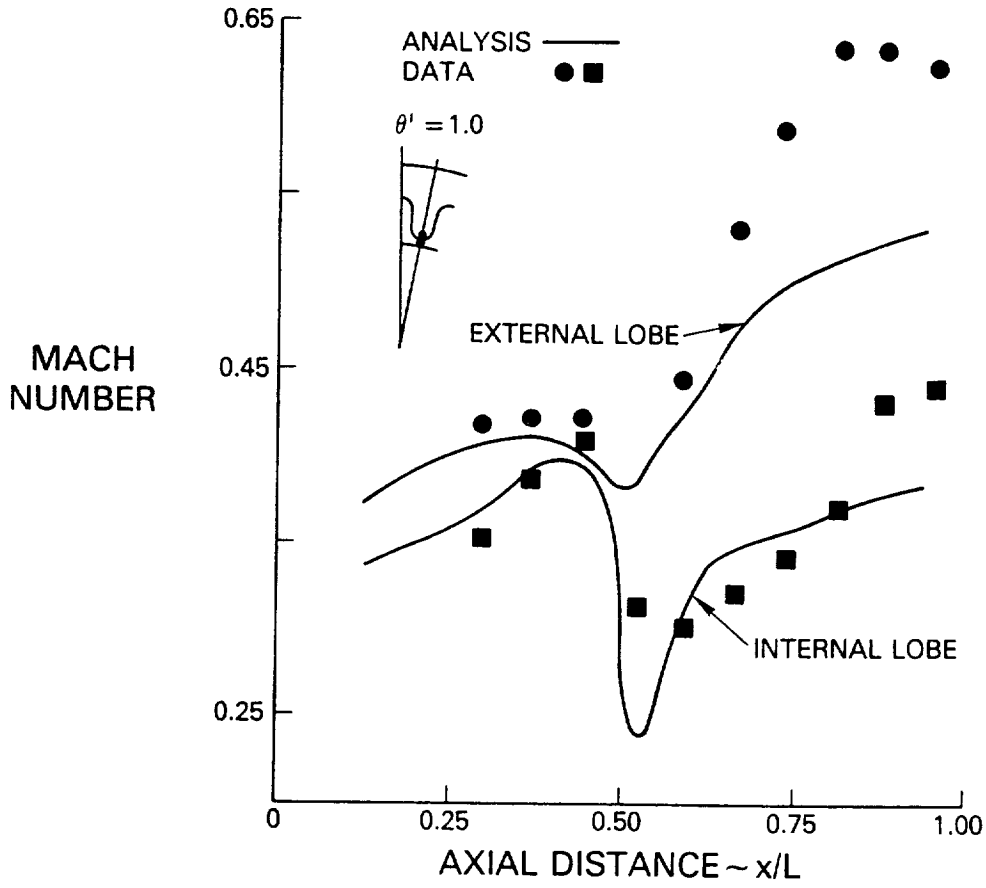

Figure 19 Surface Mach Number Comparisons for E^3 Mixer Lobe at Lobe Trough Orientation

Surface Mach number calculations, compared to measured data within the lobe region, are shown on Figs. 16-19. Figures 16, 17 present comparisons made for an azimuthal cut aligned to the lobe crest while Figs. 18, 19 show comparisons for the lobe trough orientation. Initial calculations indicated that the quasi-one-dimensional boundary condition set the flow and inlet conditions approximately 10 percent too high, therefore, a nozzle flow coefficient (C_v = 0.94) was introduced to adjust the inlet flow conditions. With this modification, the figures show substantial agreement between analysis and data. The axisymmetric fan nozzle and centerbody comparisons shown on Figures 16 and 18 show little angular variation and are largely one dimensional in behavior. The lobe surface solutions, however, show substantial θ dependence. A major discrepancy is noted near X/L = 0.50, the cross-over point for the fan and core flows. A Mach number pulse at this point is produced primarily by the first modal solution in a manner similar to Figure 12a, observed in the previously discussed planar mixer case. Viscous interaction effects should decrease the analytically predicted gradients and reduce this mismatch.

The FLOMIX analysis has also been applied to the JT8D-209 lobed mixer configuration. This configuration was previously studied at UTRC in a scaled model test but still simulating the hot flow ($\Delta P_o/P_{os}$ = 0.044, $\Delta T_o/T_{os}$ = 1.617) full scale engine cruise conditions. Analysis of this configuration

is complicated by the additional effect of a 12° scarf angle. While no surface or flowfield details were measured within the lobe region of the duct, LDV measured velocity components were obtained at the lobe trailing edge and in the mixing duct. Any analysis comparison with data, however, requires an interpretation of the small disturbance solution off the mean radius. Examination of the Mach number indicates that axial component is largely one-dimensional and has little variation with radius, within each stream. Displacing the flow relative to the physical lobe trailing edge results in comparisons for the radially measured axial component of Mach number, shown on Figure 20 at the crest location and on Figure 21 for the trough location. Both figures show substantial agreement between analysis (NH = 5, NF = 9) and experiment.

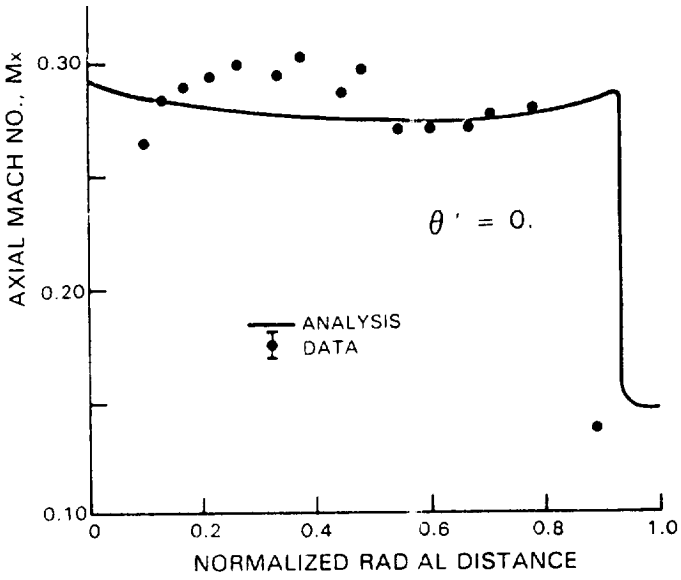

Figure 20 Comparison of Axial Mach Number at Lobe Trailing Edge Plane for JT9D-209 Mixer, Crest Orientation

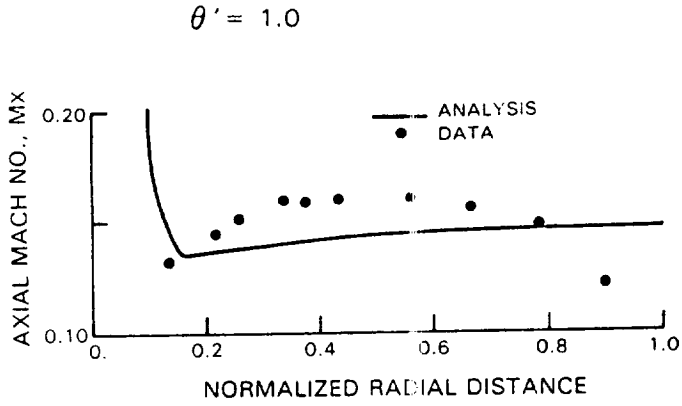

Figure 21 Comparison of Axial Mach Number at Lobe Trailing Edge Plane for JT8D-209 Mixer, Trough Orientation

A fuller interpretation of the flowfield at the lobe exit plane must be inferred from slender body theory [14,15], whereby the outer potential is determined as a function of x from the solution of an axisymmetric problem and the inner potential is determined as a solution of the two-dimensional Laplace's equation in the cross plane (r,θ). This philosophy will be used with the modal axisymmetric solutions to infer the cross flow or inner solution by viewing the potential jump as the doublet source equivalent obtained from the outer solution.

SECTION 4.0
ANALYSIS IMPLEMENTATION

A. Geometry Definition

A generalized procedure to obtain the coordinates of an arbitrary forced mixer application can be extremely complex. Although an engine centerbody is usually an axisymmetric surface, the outer cowl, which is initially also axisymmetric, can transition to a high AR rectangular cross section at the nozzle exit plane (Figure 22). Commercial applications are typically fully axisymmetric, but military applications can include such ducts. Superellipsoidal coordinates can be used to analytically approximate such circular to rectangular transition ducts.

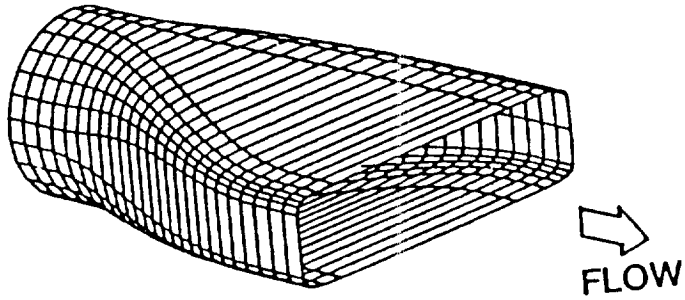

Figure 22 Engine Exhaust Transition Duct.

Lobe contour definition is however a more complex problem. Even if scalloping and scarf angle cutouts are not modelled, lobe contours can still be very general. Current commercial designs fall within three general categories; radial sidewalls, parallel sidewalls, circular are sidewalls (See Figure 23). The remaining segments of the lobe are then defined in terms of tangentially intersecting circular arc segments.

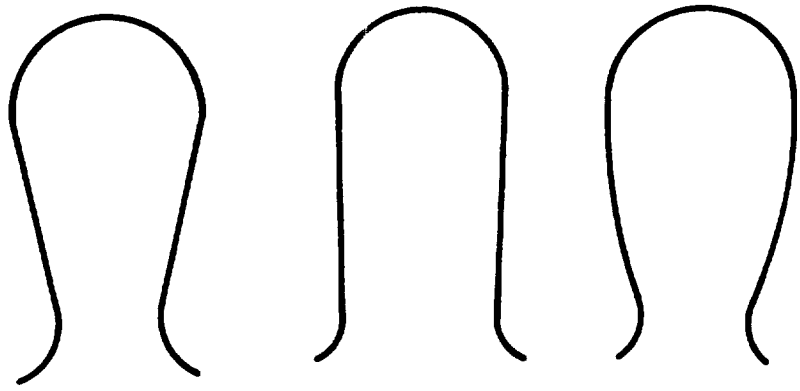

Figure 23 Typical Lobe Cross - Section Contours

Considering the periodic nature of the analysis formulated in the previous section, one must limit the geometry capability to axisymmetric duct wall configurations. The lobe cross-section must also be limited to radial sidewall geometries to avoid multiple valued structures. Lobe coordinates are analytically evaluated by dividing the lobe into three segments (shown on Figure 24).

Figure 24 Analytical Breakup of Radial Sidewall Lobe

Using this approach, the baseline JT8D-209 model 12 mixer is defined interms of the radii given on Table II, where the appropriate radii and the sectional locations are shown on Figure 25. Finally, after generating the mixer coordinates, one can replicate the lobe and display, using the BYU Movie Three-Dimensional hidden line graphics program, the lobe portion (Figure 26) as well as the complete forced mixer configuration (Figures 27, 28).

Table II - JT8D-209/12C Lobe Mixer Definition

AXIAL SECTION	A	B	C	D	E	F	G	H	I	J	K	L	M	N
X	.655	.951	1.236	1.593	1.837	2.093	2.284	2.713	3.141	3.570	3.998	4.306	4.613	5.399
$R_{Pan\ valley}$	2.729	2.719	2.694	2.642	2.593	2.517	2.449	2.276	2.103	1.929	1.756	1.632	1.508	1.190
R_{Crown}	2.503	2.503	2.503	2.503	2.526	2.593	2.662	2.831	2.994	3.105	3.160	3.167	3.146	2.997
D								.301	.313	.310	.296	.279	.258	
E	R_{FV} Tangency Radius							2.512	2.295	2.088	1.891	1.757	1.628	
F	R_{Mean}							.313	.313	.313	.313	.313	.313	
G	$R_{Mean} = [R_{FV} + R_{Crown}]/2$							2.243	2.243	2.243	2.243	2.243	2.243	
H	R_{Crown}								.299	.274	.250	.235	.233	.239
J	R Crown Tangency Radius							2.56	2.760	2.902	2.975	2.984	2.957	
K	R_{FV} Origin Radius						.963	.354	.303	.247	.207	.197	.173	
L	R Crown Origin Radius						.300	.300	.278	.255	.241	.239	.244	

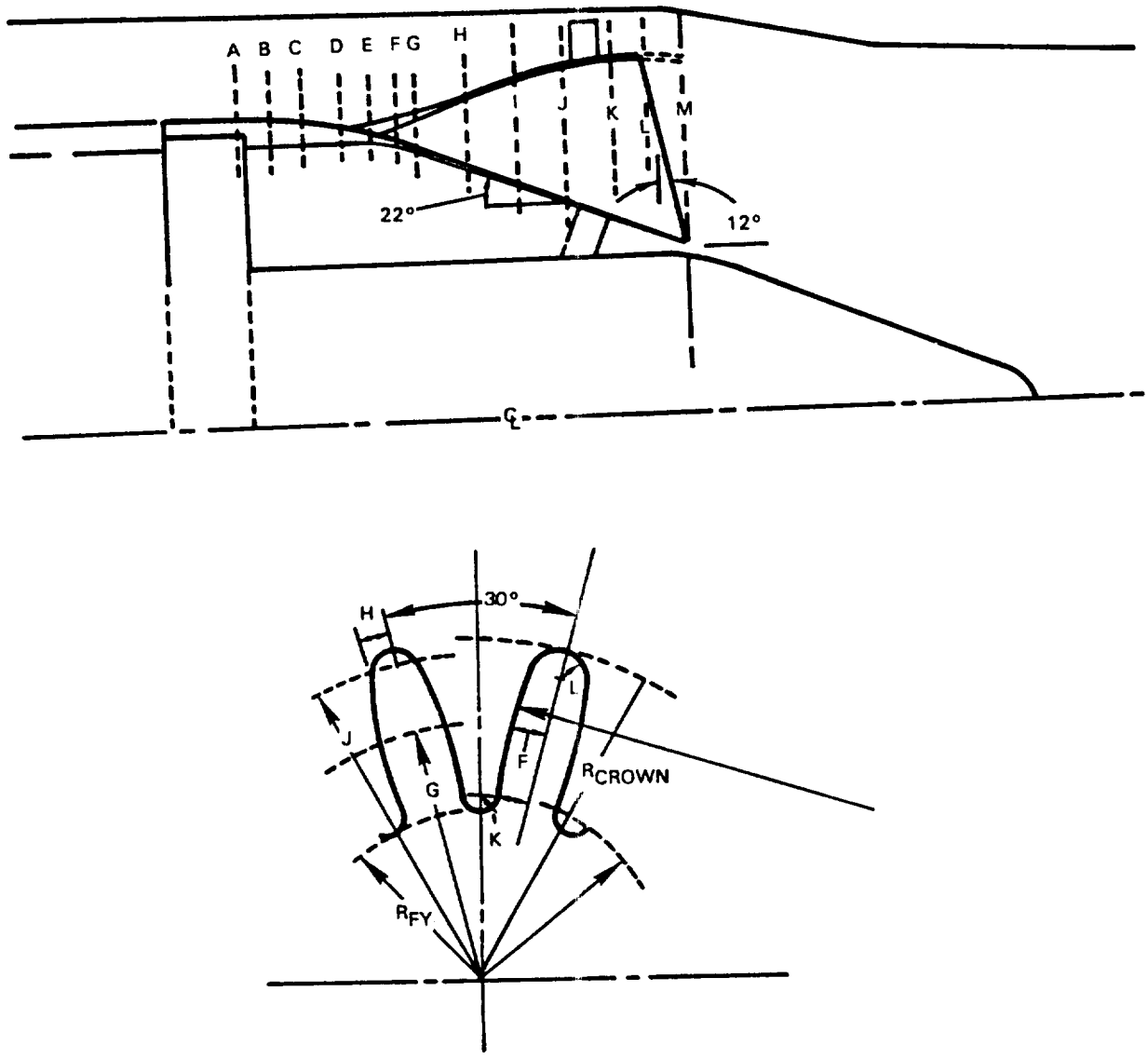

Figure 25 JT8D-209/12 mixer (-12° scarf angle) Geometry Description

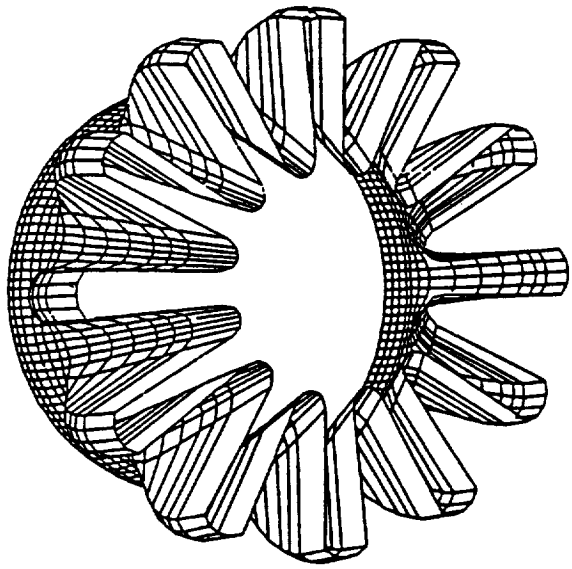

Figure 26 3-Dimensional Movie Plot of Input-Generated JT8D-209 Mixer

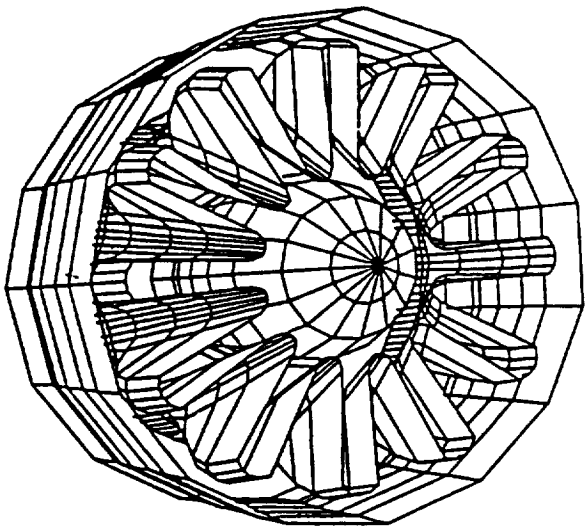

Figure 27 3-Dimensional Movie Plot of Complete JT8D-209 Mixer Geometry

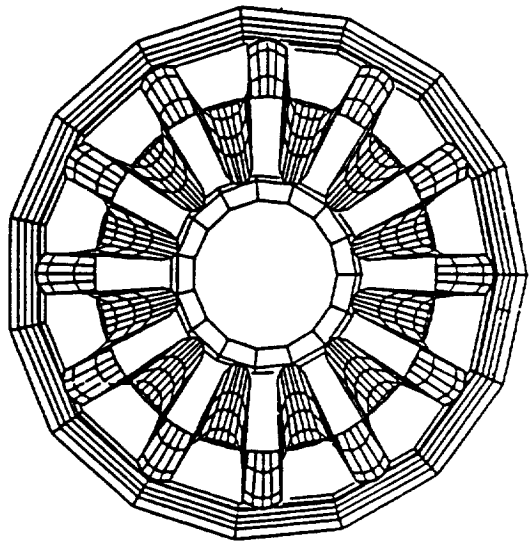

Figure 28 3-Dimensional Movie Plot of Complete JT8D-209 Mixer Geometry (Looking Upstream)

Finite Fourier Series Decomposition

Lobe contours are constructed using tangential intersection of radial lines with a variety of circular arc segments. The contours are assumed symmetric about the either the crest or trough of the lobe. The half lobe is then subdivided into NINT equal angle segments. At these points (R_j, θ_j) the lobe can be represented by a finite Fourier series, where the number of Fourier Terms is determined by the (NINT+1) constraints. A measure of the feasibility of the Fourier decomposition method formulated in Section II can be made by considering a finite number of harmonics (NH = NINT/2) and comparing the reconstructed lobe versus the lobe definition array from the given input data.

The definition of an arbitrary point on the lobe surface is given by the following series

$$F = R_j(\theta_j) = \sum_{k=0}^{NH} \left[A_k \cos(k\alpha_j) + B_k \sin(k\alpha_j) \right] + R_0$$

where

$$\alpha_j = 2\pi\theta_j / 2\theta_0 = \pi\theta_j/\theta_0 \qquad 0 \leq \theta_j \leq 2\theta_0$$

and θ_j, θ_0 are shown on the figure below.

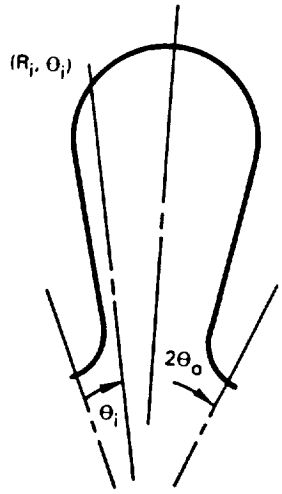

Evaluation of the unknown coefficients is possible by forming 2NH moment relations that take advantage of the orthogonality of the basic Fourier functions,
e.g.

$$\int_0^{2\pi} \Delta F \cos(i\alpha)\, d\alpha = \sum_{k=1}^{NH} \left[\int_0^{2\pi} A_k \cos(k\alpha)\cos(i\alpha)\, d\alpha + \int_0^{2\pi} B_k \sin k\alpha)\cos(id)\, d\alpha \right]$$

$$i = 0,1,2,\ldots NH$$

Using trigonometric integral identities to simplify the above equation one obtains

$$B_k = \frac{1}{\pi}\int_0^{2\pi} \Delta F \sin(k\alpha)\, d\alpha \qquad k = 0,1,2,\ldots NH$$

$$A_k = \frac{1}{\pi}\int_0^{2\pi} \Delta F \cos(k\alpha)\, d\alpha \qquad k = 0,1,2,\ldots NH$$

An equal angle series construction permits use of fast Fourier scheme (FFT) to evaluate the unknown coefficients. A more reasonable contour definition, however, can be obtained by using an equal arc length definition of the input data. In such a formulation, the coefficients must be evaluated using a more conventional matrix inversion procedure.

The truncated Fourier series has been applied to the three lobe families shown on Figure 23. The limit on angular double valuedness for the parallel and curved side wall geometrics was eliminated, only for this geometry study, by using an equal arc length decomposition of the lobe surface. The reconstructed lobes are shown on Figures 29, 30, 31 for NH = 3 and 5. The base or reference contour was generated analytically using 50 points. One can see that relatively few modes are required to produce a good surface representation of the parallel and curved side wall cases. The radial analysis however does not demonstrate the same degree of agreement. The largest excursion occurs at points where the curvature changes instantaneously. This aspect is commonly found in square wave reconstructions, where a large number of modes must be used to obtain an accurate wave representation. The relative mismatch is, however, enhanced by the magnification of the abcissa scale.

The level of error should be compared however not only to the analytic contour reference but also to the manufacturing tolerance of the mixer. Mixer lobes can be accurately fabricated by three-dimensional machining of a solid mass, however, this is prohibitively expensive. Our JT8D-200 mixer experience, also used for the JT8D benchmark mixer (Ref. 5), shows that a typical mixer can have dimensional variations as large as 0.4 inch. For example, a calibration of two adjacent lobes on the benchmark mixer (Figures 32, 33) shows substantial lobe to variation. It therefore seems reasonable that only 3-5 modes will be necessary to provide adequate three-dimensional contour and flow reconstruction. In production practice the lobe-to-lobe variations seem to compensate as long as lobe flow area is maintained.

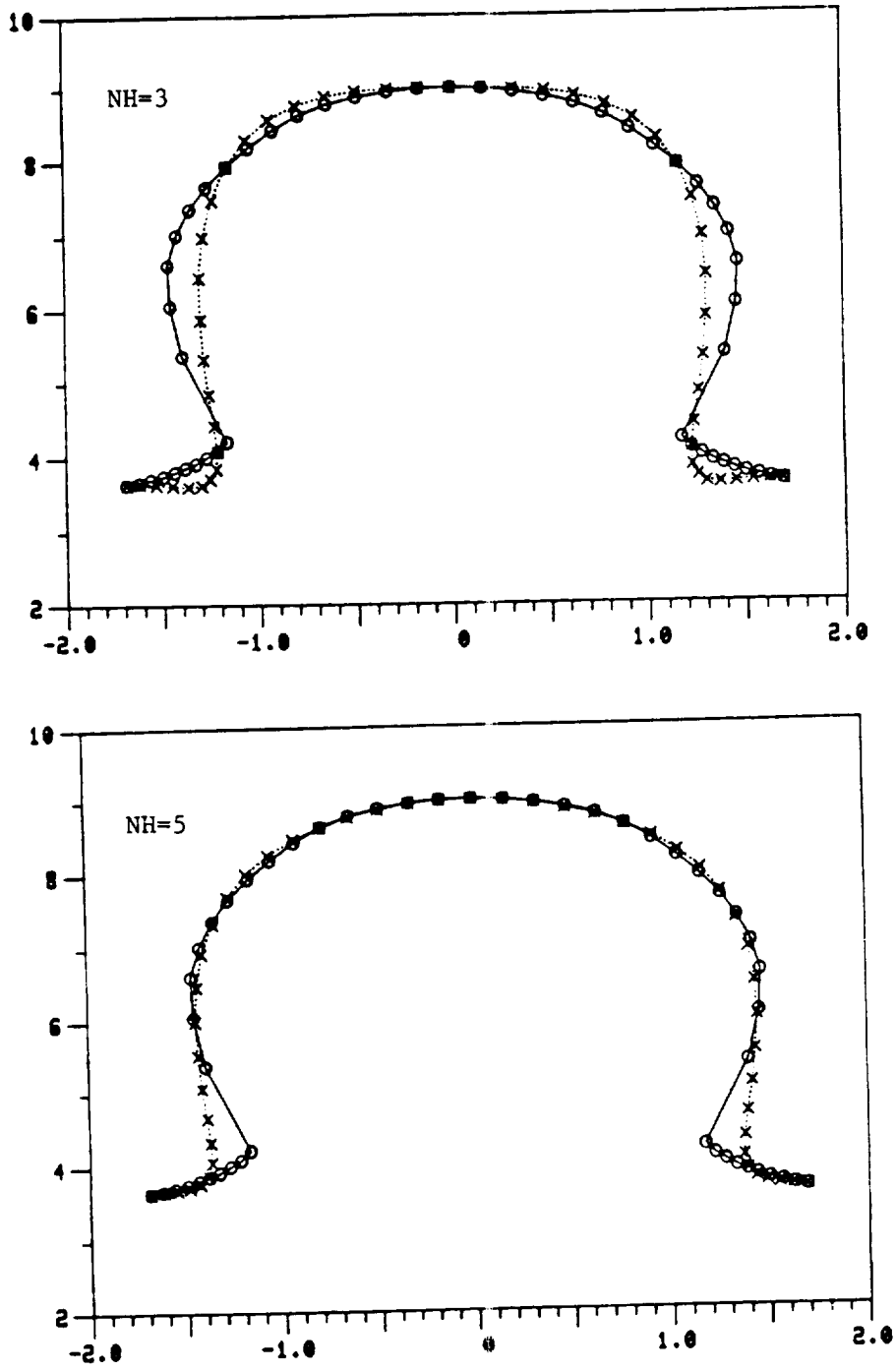

Figure 29 Comparison of Fourier Modal Reconstruction of Lobe Contour for Curved Sidewall Model of JT8D Lobe at STA 13,X/L= 93% (....X Fourier, _____o Analytic)

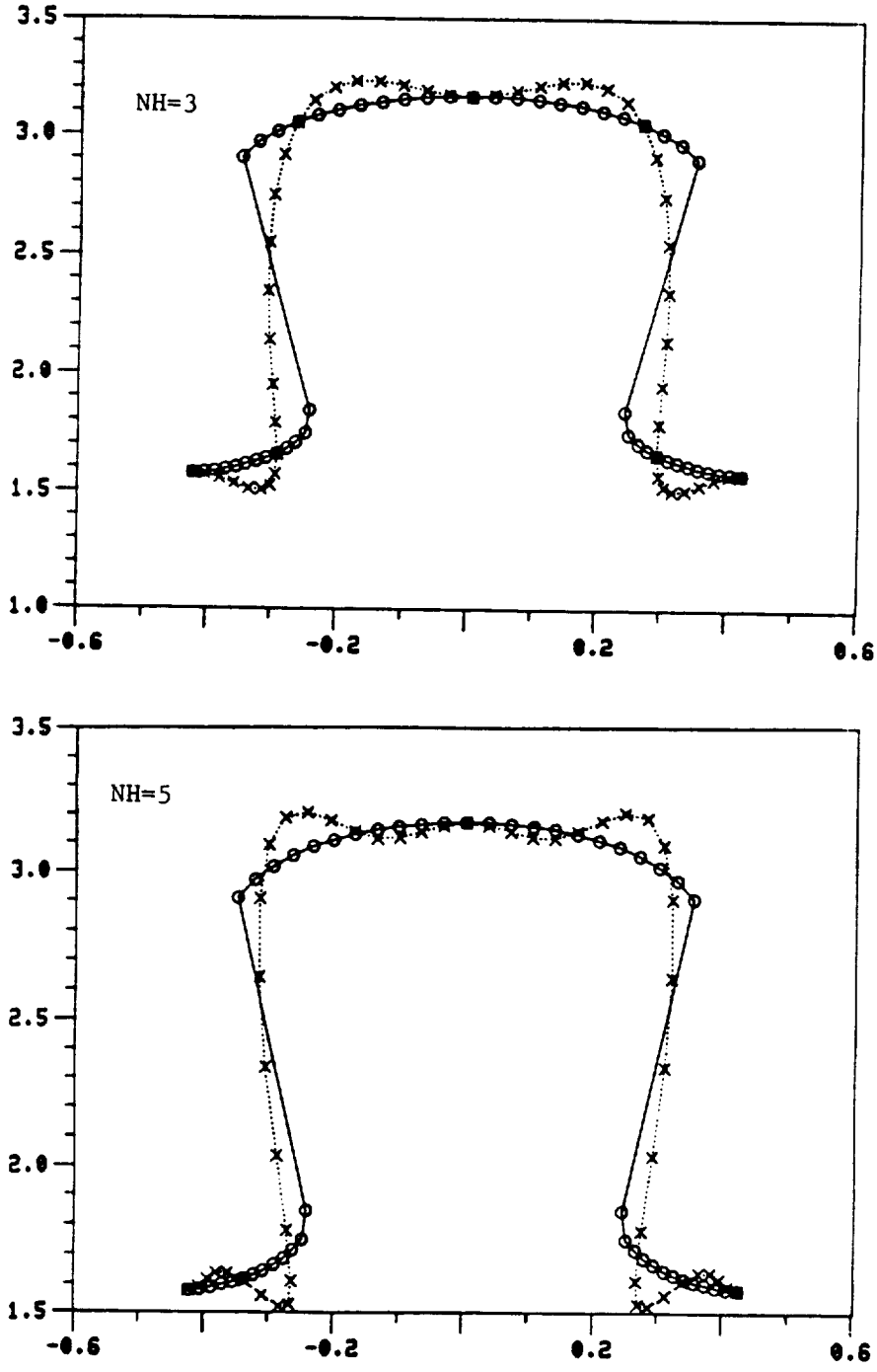

Figure 30 Comparison of Fourier Modal Reconstruction of Lobe Contour for Radial Sidewall Model of JT8D Lobe at STA 13,X/L= 93% (.....X Fourier,_____o Analytic)

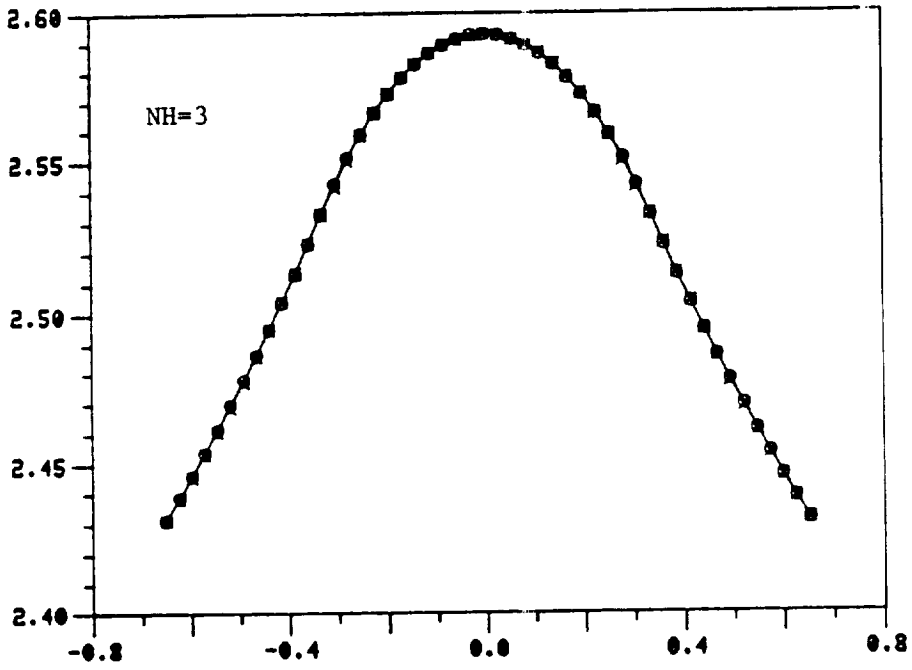

Figure 31 - Comparison of Fourier Modal Reconstruction of Lobe Contour for Radial Sidewall Model of JT8D Lobe at STA 7,X/L= 45% (...X Fourier, _____o Analytic)

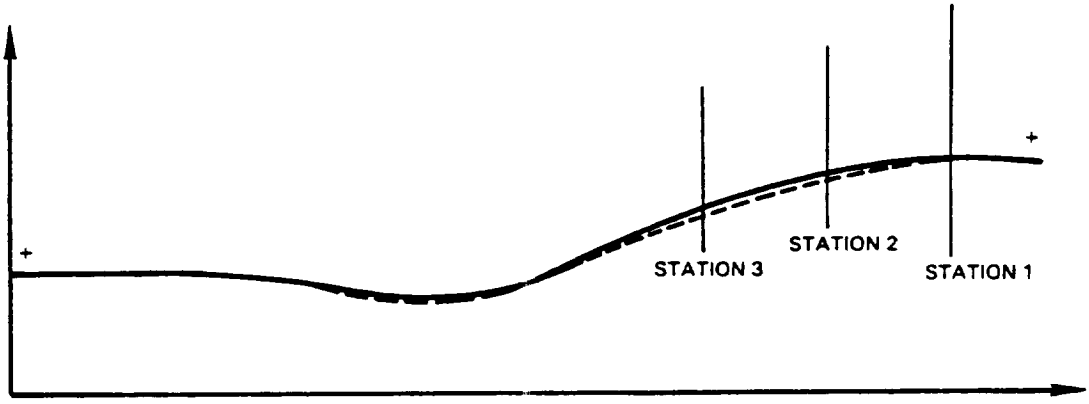

Figure 32 Axial Profile JT8D-209 Baseline Mixer

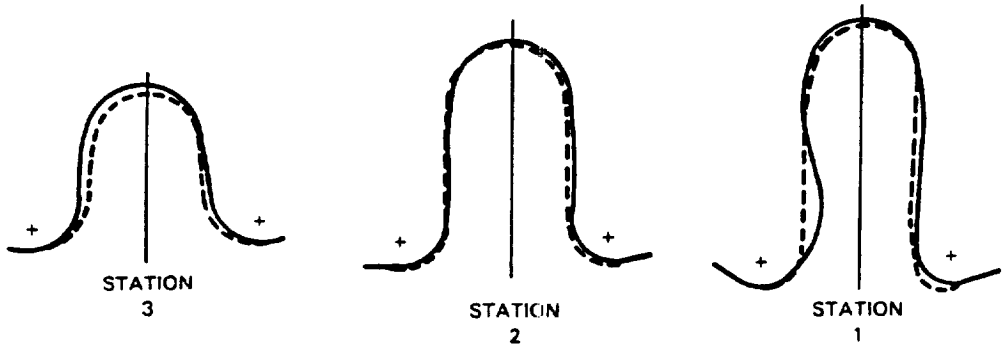

Figure 33 Circumferential Profile of JT8D-209 Baseline Mixer

B. Linking Diagram for FLOMIX Program

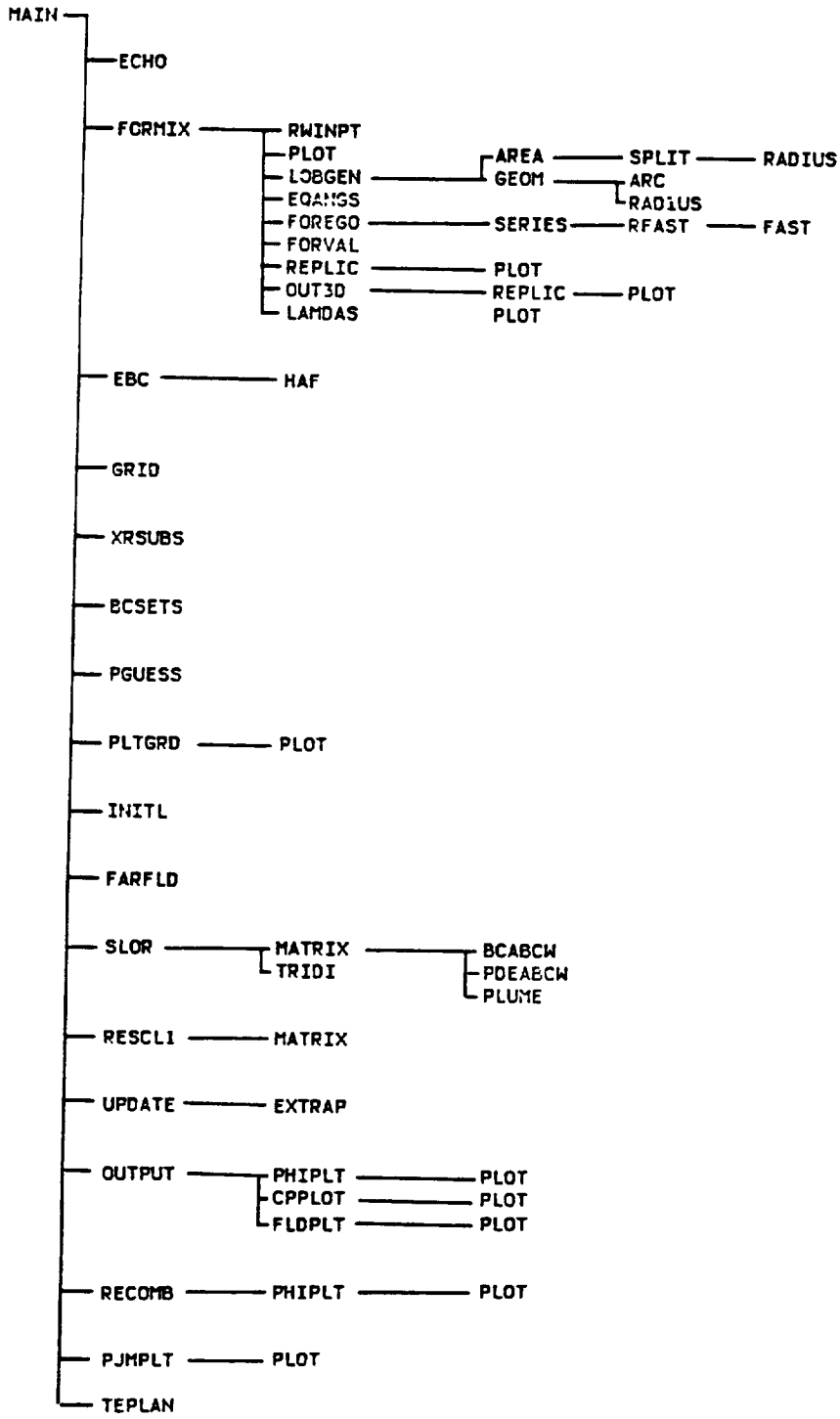

C. Input Description for FLOMIX Program

The format of each input item is identified by type.

Type	Example	Description
A	TEST CASE	Alphanumeric: Any keyboard characters are specified within the given field.
F	-23.64	Floating Point: Decimal fractions including decimal point are specified anywhere within the given field. Positive values are assumed unless the value is preceded by a minus sign.
	-.2364 E2	Scientific notation may be substituted by specifying a decimal mantissa (as above) and a right adjusted base 10 multiplier preceded by a symbol E.
I	42	Integer: Right adjusted whole numbers (no decimal point) are specified within the given field.

Blank F or I fields are set equal to zero, but blank A fields are set equal to blank characters.

Card Type 1

Column	Item	Type	Description
1-52	AXITLT	A	Title for plotting routine

Card Type 2

Column	Item	Type	Description
1-80	TITLE	A	Title of case for printout

Card Type 3

Column	Item	Type	Description
1-5	NLOBE	I	No. of mixer lobes
6-10	NHARM	I	No. of harmonic solutions

Card Type 4

Column	Item	Type	Description
1-10	PT1	F	Total pressure of primary flow, psi
11-20	TT1	F	Total temperature of primary flow, °R
21-30	GAM1	F	γ_1, specific heat ratio of primary flow
31-40	R1	F	R_1, gas constant of primary flow ft=lb/lbm-°R
41-50	P1NF	F	Static pressure of external or ambient flow, psi

Card Type 5

Column	Item	Type	Description
1-10	PT2	F	Total pressure of fan flow, psi
11-20	TT2	F	Total temperature of fan flow, °R
21-30	GAM2	F	γ_2, specific heat ratio of fan flow
31-40	R2	F	R_2, gas constant of fan flow, ft-lb/lbm-°R

Card Type 6

Column	Item	Type	Description
1-5 mesh	IMXFIN	I	No. of axial (I) grid lines on finest
6-10 mesh	JMXFIN	I	No. of radial (J) grid lines on finest
11-20	XMIN	F	X_{min}, minimum axial grid location
21-30	XMAX	F	X_{max}, maximum axial grid location
31-40	RMIN	F	*R_{min}, minimum radial grid location
41-50	RMAX	F	*R_{max}, maximum radial grid location

*Coordinate data for centerbody and fan cowl geometries must be specified within these radial grid limits.

Card Type 7

Maximum of five grid halvings are possible, with last being on finest mesh. Setting NGRIDS=1 will calculate only on finest mesh.

Column	Item	Type	Description
1-5	NGRIDS	I	No. of grids used in mesh halving
6-10	MAXSWP(1)	I	Maximum No. sweeps on grid 1 without satisfying its convergence tol.
11-15	MAXSWP(2)	I	Maximum No. sweeps on grid 2
16-20	MAXSWP(3)	I	Maximum No. sweeps on grid 3
21-25	MAXSWP(4)	I	Maximum No. sweeps on grid 4
26-30	MAXSWP (NGRIDS)	I	Maximum No. sweeps on grid 5

Card Type 8

Column	Item	Type	Description
1-10	RLXSUB	F	Over Relaxation factor for SLOR (Recommended=1.7)
11-20	PHIXT	F	Factor controlling ϕx_t artificial time term
21-30	PHIR	F	Factor controlling ϕ_t artificial time term

Card Type 9

Extrapolated Relaxation Parameters (Set to zero for no extrapolation)

Column	Item	Type	Description
FREE FORMAT	INSTEP	I	Minimum No. iteration sweeps before forced extrapolation (default=250)
	INDJMP	I	Minimum No. iteration sweeps between extrapolation cycles (default=25)
	TOLJMP	F	Tolerance factor (default=1.5)
	NSWAVE	I	No. of sweeps used in calculating average residual for extrapolation (default=5)

Card Type 10

Output control parameters

Column	Item	Type	Description
1-5	IDUMP	I	=0, Minimum output (Input, Fourier analysis, surface Cp) =1, + Surface Mach No. =2, + surface g's =3, + diagnostic output dump
6-10	NTH	I	Number of azimuthal output planes at lobe trailing edge
11-15	NR	I	Number of radial output points at lobe trailing edge
16-20	IPLOT	I	=0, No output plots =1, Summary plots =2, + Final grid Cp solution =3, + potential and Cp for all grids

Card Type 11

Specify NSTA cards of input data (Program will read to end of file)

Column	Item	Type	Description
1-10	STA(I)	I	Axial Station, in
11-20	RID(I)	I	RID, Centerbody/plug radius, in.
21-30	REL(I)	I	R crown, lobe crown or maximum radius, in.
31-40	ROD(I)	I	ROD, Fan cowl radius, in.
41-50	RFV(I)	I	RFV, lobe fan valley or minimum radius, in.
51-60	XPCNT(I)	I	α/θ , Percent of half lobe angle to radial side-wall plane (input some dummy value for axisymmetric problems)

D. Sample Input (JT8D-209 Forced Mixer)

```
INPUT ECHO (CARD IMAGE)
                                10        20        30        40        50        60        70        80
              COL  123456789 123456789 123456789 123456789 123456789 123456789 123456789 123456789

         1              FLOMIX TEST CASE
         2            JT8D MIXER NOZZLE SMOOTHED DATA (46 EQUALLY SPACED POINTS)
         3             12    6
         4                38.1    1360.0       1.4      53.3      14.5
CARD     5                36.5     519.7       1.4      53.3       1.0
         6            129  129      0.0      10.0               4.3
         7              3  500  400  300
         8             1.50
         9              0    0    0    0.0
CARD    10              1    9   20
        11             0.30000   1.37000   2.50308   3.59941   2.72835   .5
        12             0.50000   1.37000   2.50220   3.60273   2.73194   .5
        13             0.70000   1.37000   2.49995   3.59808   2.73019   .5
        14             0.90000   1.37000   2.49682   3.58596   2.72254   .5
CARD    15             1.10000   1.37000   2.49372   3.56682   2.70907   .5
        16             1.30000   1.37000   2.49210   3.54987   2.68888   .5
        17             1.50000   1.37000   2.49592   3.53214   2.66104   .5
        18             1.70000   1.37000   2.50770   3.51697   2.62474   .5
        19             1.90000   1.37000   2.54077   3.50459   2.57560   .5
CARD    20             2.10000   1.37000   2.60664   3.49427   2.51038   .5
        21             2.30000   1.37000   2.68890   3.48539   2.43535   .5
        22             2.50000   1.37000   2.76950   3.47558   2.35800   .5
        23             2.70000   1.37000   2.84437   3.46476   2.27979   .5
        24             2.90000   1.37000   2.91311   3.45240   2.20069   .5
CARD    25             3.10000   1.37000   2.97525   3.43847   2.12076   .5
        26             3.30000   1.37000   3.03044   3.42368   2.04014   .5
        27             3.50000   1.37000   3.07743   3.40714   1.95911   .5
        28             3.70000   1.37001   3.11496   3.39006   1.87790   .5
        29             3.90000   1.37027   3.14233   3.37188   1.79665   .5
CARD    30             4.10000   1.36046   3.15891   3.35311   1.71544   .5
        31             4.30000   1.33175   3.16393   3.33430   1.63440   .5
        32             4.50000   1.29293   3.15617   3.31538   1.55361   .5
        33             4.61300   1.26135   3.14600   3.30470   1.50800   .5
        34             4.90000   1.15748   0.0       3.27834   0.0       .5
CARD    35             5.10000   1.08316   0.0       3.26075   0.0       .5
        36             5.30000   1.00883   0.0       3.24317   0.0       .5
        37             5.50000   0.93437   0.0       3.22710   0.0       .5
        38             5.70000   0.85979   0.0       3.21132   0.0       .5
        39             5.90000   0.78520   0.0       3.19571   0.0       .5
CARD    40             6.10000   0.71067   0.0       3.18172   0.0       .5
        41             6.30000   0.63636   0.0       3.16774   0.0       .5
        42             6.50000   0.56219   0.0       3.15439   0.0       .5
        43             6.70000   0.48860   0.0       3.14216   0.0       .5
        44             6.90000   0.41623   0.0       3.12992   0.0       .5
CARD    45             7.10000   0.34448   0.0       3.11836   0.0       .5
        46             7.30000   0.27501   0.0       3.10742   0.0       .5
        47             7.50000   0.20645   0.0       3.09663   0.0       .5
        48             7.70000   0.13948   0.0       3.08634   0.0       .5
        49             7.90000   0.07433   0.0       3.07611   0.0       .5
CARD    50             8.10000   0.01003   0.0       3.06597   0.0       .5

              COL  123456789 123456789 123456789 123456789 123456789 123456789 123456789 123456789
                          10        20        30        40        50        60        70        80
```

E. Subroutine Definition for FLOMIX Program

```
C*****************************************************************
C
C
C  WELCOME TO FLOMIX, THE AXISYMMETRIC POTENTIAL FLOW ANALYSIS. THE
C  GUDERLEY-VON KARMAN TRANSONIC SMALL DISTURBANCE EQUATION IS THE
C  GOVERNING PARTIAL DIFFERENTIAL EQUATION. THE DISCRETIZED
C  FORMULATION IS BASED ON A FINITE VOLUME CONSERVATION OF MASS
C  FLUXES. THE BOUNDARY CONDITIONS ARE APPLIED ON THE EXACT SURFACE.
C  A NONCONSERVATIVE SHOCK POINT OPERATOR IS AVAILABLE IN LIEU OF
C  THE DEFAULT CONSERVATIVE OPERATOR. THE CONFIGURATIONS WHICH
C  CAN BE ANALYSED INCLUDE STING-MOUNTED OR FINITE LENGTH NACELLES
C  WITH OR WITHOUT A CENTERBODY. BOTH FREESTREAM OR WIND TUNNEL
C  CONDITIONS CAN BE SIMULATED. AN ACTUATOR DISK MODEL IS USED TO
C  SIMULATE POWER ADDITION TO THE FLOW. GRID REFINEMENT AND
C  EXTRAPOLATION TECHNIQUES ARE USED TO ACCELERATE CONVERGENCE.
C
C  THE MAIN ROUTINE CONTAINS THE BASIC STRUCTURE OF THE PROGRAM.
C
C  ROUTINES CALLED:
C    ECHO   - ECHOS CARD IMAGE INPUT
C    FORMIX - READS THE SPECIFIED DATA FILE, OR HELPS THE USER CREATE
C             A NEW DATA FILE WHEN ONLY THE CONTOUR IS GIVEN.
C    EBC    - CALCULATES THE POSITION OF THE DOWNSTREAM BOUNDARY AND THE
C             DOWNSTREAM MACH NUMBERS FOR EACH STREAM.
C    GRID   - GENERATES A CARTESIAN MESH FOR THE DENSEST GRID.
C    XRSUBS - GENERATES COARSE GRID SUBSETS OF THE DENSEST GRID,
C             AS WELL AS CALCULATING COARSE GRID VALUES OF VARIABLES
C             SUCH AS IMAX, JMAX, IH, AND ITE.
C    BCSETS - GENERATES THE ARRAYS WHICH ARE USED TO ESTABLISH THE
C             EXACT SURFACE BOUNDARY CONDITIONS.
C    PGUESS - GENERATES AN INITIAL GUESS FOR THE POTENTIAL, PHI. THE
C             GUESS IS OBTAINED EITHER FROM A SAVED SOLUTION, THE
C             SOLUTION FROM THE PREVIOUS GRID, OR A GIVEN FUNCTIONAL
C             FORM.
C    INITL  - SETS UP INITIALIZATION FOR EXTRAPOLATED RELAXATION
C    FARFLD - GENERATES THE FAR FIELD BOUNDARY CONDITIONS. THIS
C             SUBROUTINE IS INCLUDED IN THE RELAXATION SWEEPING LOOP TO
C             ALLOW FOR PERIODIC UPDATING BASED ON THE CIRCULATION.
C    SLOR   - PERFORMS A SUCCESSIVE LINE OVER-RELAXATION. FOR
C             EACH COLUMN IN THE CARTESIAN MESH, A TRIDIAGONAL MATRIX
C             IS SET UP AND SOLVED. THE CORRECTIONS ARE APPLIED WITH
C             AN OVER-RELAXATION FACTOR FOR SUBSONIC FLOW, AND AN
C             UNDER-RELAXATION FACTOR FOR SUPERSONIC FLOW. WHEN
C             THE PROPER CRITERIA ARE MET, AN EXTRAPOLATION IS CALLED.
C    UPDATE - UPDATES CORRECTIONS FOR NEXT SWEEP THROUGH RELAXATION LOOP
C    RESCL1 - CALCULATES RESIDUES FOR EACH SWEEP THROUGH RELAXATION LOOP
C    OUTPUT - CALLS THE VARIOUS OUTPUT SUBROUTINES THAT APPLY
C             TO EACH GRID. THESE INCLUDE THE CP PLOTS, THE MASS
C             FLOW INTEGRATIONS, AND THE DRAG CALCULATION.
C    FINISH - PROVIDES A SUMMARY OF THE ANALYSIS, AND WRITES
C             INFORMATIONS TO A FILE FOR FUTURE CALCULATIONS.
C    RECOMB - RECOMBINES EACH HARMONIC SOLUTION INTO ONE SOLUTION
C    PJMPLT - PLOTS THE JUMP IN PHI OVER ALL ITERATIONS
C
C  ROUTINES CALLED BY:
C
C


C*****************************************************************
      SUBROUTINE ECHO
C
C    CARD IMAGE INPUT ECHO
C
C    ROUTINES CALLED BY:
C      FLOMIX PROGRAM
C
```

```
C*************************************************************
      SUBROUTINE FORMIX(THE,AXITLT)
C
C  FORMIX DOES THE FOLLOWING:
C    (1) READS THE LOBE CROSS-SECTION GEOMETRY DATA FROM R. WILEY'S
C        PROGRAM.
C    (2) FORMS A SERIES OF POINTS AT EQUAL INTERVALS OF ANGLE PHI
C        TO DEFINE THE LOBE CROSS-SECTION FOR FOURIER DECOMPOSITION.
C    (3) FORMS A FOURIER DECOMPOSITION OF A SELECTED CROSS-SECTION.
C    (4) RECREATES THE MIXER CROSS-SECTION USING A SELECTED NUMBER OF
C        TERMS OF THE FOURIER EXPANSION.
C    (5) GIVES A TEKTRONIX SCOPE PICTURE OF THE MIXER CROSS-SECTION
C        AND THE FOURIER REPRESENTATION.
C    (6) CALCULATES A TABLE OF THE MIXER CROSS-SECTION VALUES,
C        CORRESPONDING FOURIER VALUES, ABSOLUTE ERRORS BETWEEN
C        CORRESPONDING VALUES, AND GIVES THE RMS ERROR AND MAX. ABS.
C        ERROR FOR THE CROSS-SECTION.
C
C  OUTPUT ARGUMENTS:
C    THE    - THETA ANGLES
C    AXITLT - PLOT TITLE
C
C  ROUTINES CALLED:  LOBGEN, EQANGS, FOREGO, FORVAL, RWINPT, REPLIC,
C                    OUT3D, LAMDAS
C    LOBGEN - CALCULATES MIXER LOBE SHAPES AND CROSS SECTIONS
C    EQANGS - COMPUTES THE SERIES OF (Z,Y) PAIRS WHICH DESCRIBE THE
C             SHAPE OF A DIFFUSER LOBE FOR A FOURIER DECOMPOSITION OF
C             THE SHAPE INTO ITS FREQUENCY REPRESENTATION.
C    FOREGO - COMPUTES THE COEFFICIENTS OF THE FOURIER SERIES
C             REPRESENTATION OF R VS. ARC.  ONE LOBE OF A DIFFUSER
C             CROSS-SECTION IS THUS APPROXIMATED FROM PHI=-THETA TO
C             PHI=THETA.
C    FORVAL - COMPUTES THE VALUE OF A FOURIER SERIES AT ARCS USING NTERM
C             TERMS IN THE EXPANSION
C    RWINPT - PERFORMS READING OR WRITING OF USER INPUT
C    REPLIC - REPLICATES THE SINGLE LOBE REPRESENTATIVE INTO A MIXER
C             CROSS-SECTIONAL VIEW
C    OUT3D  - CREATES 3D OUTPUT FILE FOR 'MOVIE' PLOTTING
C    LAMDAS - CALCULATES AND PLOTS LAMBDAS AND LAMBDA PRIMES
C
C  ROUTINES CALLED BY:
C    FLOMIX PROGRAM
C*************************************************************
      SUBROUTINE RWINPT(AXITLT,XPCNT,STA,ISHAPE,ALF,THE,EY,EZ,RE,FY,FZ,
                        RF,IRWOPT)
C
C   THIS SUBROUTINE PERFORMS READING OR WRITING OF USER INPUT.
C
C   INPUT AND OUTPUT ARGUMENTS:
C     AXITLT,XPCNT,STA,ISHAPE,ALF,THE,EY,EZ,RE,FY,FZ,RF
C     IRWOPT - READ/WRITE OPTION
C              = 0, READ
C              = 1, WRITE
C
C   ROUTINES CALLED BY:
C     FORMIX - READS THE SPECIFIED DATA FILE, OR HELPS THE USER CREATE
C              A NEW DATA FILE WHEN ONLY THE CONTOUR IS GIVEN.
C*************************************************************
      SUBROUTINE OUT3D(XFF,YFF,ZFF,PF,IANL,NSTA,NTOTL)
C
C  CREATES 3D OUTPUT FILE FOR 'MOVIE' PLOTTING
C
C  INPUT ARGUMENTS:
C    XFF   - X COORDINATES
C    YFF   - Y COORDINATES
C    ZFF   - Z COORDINATES
C    PF    - COMPLEX ARRAY FOR Y AND Z
C    IANL  - ARRAY IDENTIFYING STATIONS THAT WERE ANALYZED
C    NSTA  - NO. OF STATIONS
C    NTOTL - NO. OF POINTS ABOUT A LOBE
C
C  ROUTINES CALLED:
C    REPLIC - REPLICATES THE SINGLE LOBE REPRESENTATIVE INTO A MIXER
C             CROSS-SECTIONAL VIEW
C
C  ROUTINES CALLED BY:
C    FORMIX
```

```
C*************************************************************
      SUBROUTINE AREA(X0,W,APRI,AFAN,AGAP,PEN,NLOBE,NST,IERR)
C
C  THIS SUBROUTINE CALCULATES MIXER AREA ON A NON-VERTICAL PLANE
C  DEFINED BY THE X AXIS INTERCEPT, X0, AND ANGLE, W.
C  NOTE:  POSITIVE W IS CCW FROM VERTICAL.
C
C  INPUT ARGUMENTS:
C    X0    - X AXIS INTERCEPT
C    W     - ANGLE
C    NLOBE - NO. OF LOBES
C    NST   - NO. OF LOBE STATIONS
C
C  OUTPUT ARGUMENTS:
C    APRI  - PRIMARY AREA
C    AFAN  - FAN VALLEY AREA
C    AGAP  - GAP AREA
C    PEN   - AMIX / ATOT
C    IERR  - ERROR CODE (0-NO ERROR, 1-ERROR)
C
C  ROUTINES CALLED:
C    SPLIT  - DETERMINES THE INTERSECTION OF A PLANE DEFINED BY
C             X-INTERCEPT, X0, AND ANGLE, W., AND A SPLINE FIT CURVE
C             DEFINED FROM VALUE OF IND.
C
C  ROUTINES CALLED BY:
C    LOBGEN - CALCULATES MIXER LOBE SHAPES AND CROSS-SECTIONS
C
C*************************************************************
      SUBROUTINE SPLIT(X0,W,IND,X1,R ,NST)
C
C  THIS SUBROUTINE DETERMINES THE INTERSECTION OF A PLANE
C  DEFINE BY X INTERCEPT, X0, AND ANGLE, W., AND A SPLINE
C  FIT CURVE DEFINED FROM VALUE OF IND.
C  IND IS USED IN FUNCTION RADIUS(X,IND,R) AS AN INDICATOR
C  OF WHICH SPLINE FIT IS TO BE READ.
C
C  INPUT ARGUMENTS:
C    X0  - X INTERCEPT
C    W   - ANGLE
C    IND - SPLINE FIT INDICATOR
C    NST - NO. OF LOBE STATIONS
C
C  OUTPUT ARGUMENTS:
C    X1  - X INTERSECTION
C    R1  - INTERSECTION RADIUS
C
C  ROUTINES CALLED:
C    RADIUS - EVALUATES SPLINE FIT CURVES AT SPECIFIED LOCATIONS
C
C  ROUTINES CALLED BY:
C    AREA   - CALCULATES MIXER AREA ON A NON-VERTICAL PLANE DEFINED
C             BY THE X AXIS INTERCEPT, X0, AND ANGLE, W.
C
C*************************************************************
      REAL FUNCTION ZPRI(X,Y)
C
C  THIS FUNCTION EVALUATES MIXER PRIMARY LOBE WIDTH AT AXIAL STATION X
C  AND HEIGHT Y.
C  USED AS F(X) FOR SIMPSON(S RULE INTEGRATION.
C
C  INPUT ARGUMENTS:
C    X    - AXIAL STATION
C    Y    - HEIGHT
C
C  OUTPUT ARGUMENTS:
C    ZPRI - MIXER PRIMARY LOBE WIDTH
C
C  ROUTINES CALLED:
C    GEOM - CALCULATES VERTICAL SECTION GEOMETRY
C
C  ROUTINES CALLED BY:
C    AREA - CALCULATES MIXER AREA ON A NON-VERTICAL PLANE DEFINED BY
C           THE X AXIS INTERCEPT, X0, AND ANGLE, W.
C
```

```
C*************************************************************
      SUBROUTINE LOBGEN(STA,RID,REL,RFV,ROD,XPCNT,NST,ITRANS,ALF,THET,
                        BYY,BZZ,RBB,CYY,CZZ,RCC)
C
C  RADIAL WALL MIXER DECK - OBTAINED FROM D. WILEY (2-23-83)
C
C  THIS ROUTINE CALCULATES MIXER LOBE SHAPES AND CROSS-SECTIONS.
C
C  INPUT ARGUMENTS:
C    STA     - STATION X VALUES
C    RID     - PLUG RADIUS
C    REL     - ENGINE LOBE RADIUS
C    RFV     - FAN VALLEY RADIUS
C    ROD     - OUTER CASE RADIUS
C    XPCNT   - LOBE ANGLE PERCENTAGE
C    NST     - NO. OF STATIONS
C
C  OUTPUT ARGUMENTS:
C    ITRANS - MIXER SHAPE AT EACH AXIAL STATION
C    ALF     - ANGLE TO MIXER WALL
C    THET    - ANGLE OF HALF A LOBE
C    BYY     - Y COORDINATE OF CENTERPOINT OF LOBE
C    BZZ     - Z COORDINATE OF CENTERPOINT OF LOBE
C    RBB     - RADIUS OF THE LOBE
C    CYY     - Y COORDINATE OF CENTERPOINT OF FAN VALLEY
C    CZZ     - Z COORDINATE OF CENTERPOINT OF FAN VALLEY
C    RCC     - RADIUS OF FAN VALLEY
C
C  ROUTINES CALLED:
C    BMFIT   - SPLINE FITS MIXER LINES
C    GEOM    - CALCULATES VERTICAL SECTION GEOMETRY
C    AREA    - CALCULATES MIXER AREA ON A NON-VERTICAL PLANE
C
C  ROUTINES CALLED BY:
C    FORMIX
```

```
      SUBROUTINE GEOM (X,STA,RID,REL,RFV,ROD,XPCNT,ISTA,ITRANS,IERR)
C
C  THIS ROUTINES CALCULATES VERTICAL SECTION GEOMETRY.
C
C  INPUT ARGUMENTS:
C    X       - AXIAL STATION TO BE EXAMINED
C    STA     - STATION X VALUES
C    RID     - PLUG RADIUS
C    REL     - ENGINE LOBE RADIUS
C    RFV     - FAN VALLEY RADIUS
C    ROD     - OUTER CASE RADIUS
C    XPCNT   - LOBE ANGLE PERCENTAGE
C    ISTA    - NO. OF STATIONS
C
C  OUTPUT ARGUMENTS:
C    ITRANS - MIXER SHAPE AT STATION X
C    IERR    - ERROR INDICATOR
C
C  ROUTINES CALLED:
C    BEVALE - EVALUATES BMFIT SPLINES
C    ARC     - CALCULATES VALUES FOR LOBE RADIUS, FAN VALLEY RADIUS, AND
C              THE HEIGHT OF THE FAN VALLEY.
C    RADIUS - EVALUATES SPLINE FIT CURVES AT SPECIFIED LOCATION
C
C  ROUTINES CALLED BY:
C    LOBGEN - CALCULATES MIXER LOBE SHAPES AND CROSS-SECTIONS.
C
```

```
      SUBROUTINE ARC (RS,RFAN)
C
C  GIVEN THE SIDE VIEW ENGINE LOBE HEIGHT, RELI, AND A POINT
C  ON THE RADIAL WALL, RS, WHERE THE ENGINE LOBE RADIUS, RBI,
C  AND THE FAN VALLEY RADIUS, RCI, MUST BE TANGENT, THIS ROUTINE
C  CALCULATES THE VALUES FOR RBI AND RCI, AND THE HEIGHT OF THE
C  FAN VALLEY, RFAN.
C
C  INPUT ARGUMENTS:
C    RS   - POINT ON RADIAL WALL
C
C  OUTPUT ARGUMENTS:
C    RFAN - HEIGHT OF FAN VALLEY
C
C  ROUTINES CALLED:
C
C  ROUTINES CALLED BY:
C    GEOM - CALCULATES VERTICAL SECTION GEOMETRY
C
```

```
      REAL FUNCTION RADIUS(XIN,IND,STA,RID,REL,RFV,ROD,XPCNT,ISTA)
C
C  THIS FUNCTION EVALUATES SPLINE FIT CURVES AT XIN.
C  IND IS USED AS INDICATOR DEFINING CURVE IDENTITY
C
C  INPUT ARGUMENTS:
C    XIN    - X VALUE AT WHICH SPLINE FIT CURVES ARE EVALUATED
C    IND    - INDICATOR DEFINING CURVE IDENTITY
C    STA    - STATION X VALUES
C    RID    - PLUG RADIUS
C    REL    - ENGINE LOBE RADIUS
C    RFV    - FAN VALLEY RADIUS
C    ROD    - OUTER CASE RADIUS
C    XPCNT  - LOBE ANGLE PERCENTAGE
C    ISTA   - NO. OF STATIONS
C
C  ROUTINES CALLED:
C    BEVALE - EVALUATES BMFIT SPLINES
C
C  ROUTINES CALLED BY:
C    GEOM   - CALCULATES VERTICAL SECTION GEOMETRY
C
      DIMENSION STA(1),RID(1),REL(1),RFV(1),ROD(1),XPCNT(1)
      COMMON /SPLIN2/ ARID(50), BRID(50), CRID(50), DRID(50),
     2                AREL(50), BREL(50), CREL(50), DREL(50),
     3                ARFV(50), BRFV(50), CRFV(50), DRFV(50),
     4                AROD(50), BROD(50), CROD(50), DROD(50),
     5                APCNT(50), BPCNT(50), CPCNT(50), DPCNT(50)
      COMMON /SLOPE/  RIDIP, RELIP, RFVIP, RODIP
C
C-----------------------------------------------------------------------
C
C  IND = 1,  READ PLUG RADIUS
C      = 2,  READ ENGINE LOBE RADIUS
C      = 3,  READ FAN VALLEY RADIUS
C      = 4,  READ OUTER CASE RADIUS
C
```

```
C*************************************************************
      SUBROUTINE EQANGS (EOA,EAR,FOA,FAR,THETA0,ALPHA,ISIDOP,CURRAD,N,P)
C
C  THIS SUBROUTINE COMPUTES THE SERIES OF (Z,Y) PAIRS WHICH DESCRIBE THE
C  SHAPE OF A DIFFUSER LOBE FOR A FOURIER DECOMPOSITION OF THE SHAPE
C  INTO ITS FREQUENCY REPRESENTATION.
C
C  INPUT:
C    EOA    = Y-DISTANCE TO CENTER OF CIRCULAR ARC AT THE PEAK,
C    EAR    = RADIUS OF THE CIRCULAR ARC AT THE PEAK,
C    FOA    = Y-DISTANCE TO CENTER OF CIRCULAR ARC AT THE VALLEY,
C    FAR    = RADIUS OF THE CIRCULAR ARC AT THE VALLEY,
C    THETA0 = ANGLE FROM THE PEAK TO THE VALLEY,
C    ALPHA  = ANGLE TO THE END OF THE UPPER ARC AND THE START OF THE
C             LOWER ARC
C    ISIDOP = SIDE LOBE GEOMETRY OPTION
C    CURRAD = SIDE LOBE RADIUS IF CURVED GEOMETRY (ISIDOP=2)
C    N      = TOTAL NUMBER OF POINTS FROM THE PEAK TO THE VALLEY EQUAL
C             SPACED IN ARC LENGTH.
C
C  OUTPUT:
C    P(I)   = (Y,Z) PAIRS DEFINING ONE LOBE OF THE MIXER FROM
C
C  ROUTINES CALLED:
C
C  ROUTINES CALLED BY:
C    FORMIX
C
```

```
C*************************************************************
      SUBROUTINE LAMDAS(IANL)
C
C  CALCULATES AND PLOTS LAMBDAS AND LAMBDA PRIMES
C
C  INPUT ARGUMENTS:
C    IANL  - ARRAY IDENTIFYING STATIONS THAT WERE ANALYZED
C
C  ROUTINES CALLED:
C    BMFIT - PERFORMS A SPLINE FIT OF THE USER LAMBDAS
C    BEVAL - PERFORMS AN EVALUATION BASED ON THE SPLINE FIT
C
C  ROUTINES CALLED BY:
C    FORMIX
```

```
C
      SUBROUTINE FOREGO(NPL,P,ARSIN,BRCOS,AZR,BNR)
C
C  THIS SUBROUTINE COMPUTES THE COEFFICIENTS OF THE FOURIER SERIES
C  REPRESENTATION OF R VS. ARC.  ONE LOBE OF A DIFFUSER CROSS-SECTION
C  IS THUS APPROXIMATED FROM PHI=-THETA TO PHI=THETA.
C
C  INPUT:
C    NPL    = EVEN NUMBER OF DATA POINTS.
C    P(I)   = (Z,Y) PAIRS, I=1,...,NTOTL.
C
C  OUTPUT:
C    ARSIN  = (NPL/2-1) COEFFICIENTS FOR THE SINE TERMS OF THE EXPANSION
C    BRCOS  = (NPL/2-1) COEFFICIENTS FOR THE COSINE TERMS OF THE
C               EXPANSION
C    AZR    =  CONSTANT TERM IN THE SERIES.
C    BNR    =  COEFFICIENT BNZ OF BNR*COS(NTOTL/2*DELPHI), WHERE
C    DELPHI = 6.28318*(K-1)/NPL, K=1,2,...,NPL.
C
C  ROUTINES CALLED:
C    SERIES - DETERMINATION OF COEFFICIENTS IN SERIES
C
C  ROUTINES CALLED BY:
C    FORMIX
C
```

```
C
      SUBROUTINE FORVAL (NTERM,ANGL,ACOEF,BCOEF,AZ,FVAL,BNR)
C
C  THIS SUBROUTINE COMPUTES THE VALUE OF A FOURIER SERIES AT ARCS
C  USING NTERM TERMS IN THE EXPANSION.
C
C  INPUT:
C    NTERM  = NUMBER OF TERMS USED IN THE EXPANSION.
C    ANGL   = ANGLE TO BE EVALUATED
C    ACOEF(I)  = COEFFICIENT OF COSINE TERMS, I=1,...,NMAX.
C    BCOEF(I)  = COEFFICIENT OF SINE TERMS, I=1,...,NMAX.
C    AZ     = CONSTANT TERM IN THE SERIES.
C
C  OUTPUT:
C    FVAL   = VALUE OF THE EXPANSION.
C
C  ROUTINES CALLED:
C
C  ROUTINES CALLED BY:
C    FORMIX
C
```

```
C
      SUBROUTINE REPLIC (PF,NTOTL,NLOBE,IP,I3D,XF)
C
C  SUBROUTINE REPLIC REPLICATES THE SINGLE LOBE REPRESENTATION INTO
C  A MIXER CROSS-SECTIONAL VIEW.
C
C  INPUT:
C    PF(I)  = (ZF,YF) PAIRS, I=1,...,NTOTL.
C    IP     = STATION INDICATOR
C    I3D    = SINGLE OR TOTAL STATION REPLICATION INDICATOR
C    NTOTL  = NO. OF PAIRS
C    XF     = STATION LOCATIONS
C
C  ROUTINES CALLED:
C    PLTEK2
C
C  ROUTINES CALLED BY:
C    FORMIX
```

```
C
      SUBROUTINE SERIES (Y,N,AZ,A,B,AN,YY,Z,W)
C
C  DETERMINATION OF COEFFICIENTS IN SERIES
C
C  INPUT:
C    Y(K)   = INPUT VALUE OF FUNCTION AT AN ANGLE OF TK=2.*PI*(K-1)/N
C               FOR K=1 TO K=N
C               PI = 3.1415927.....
C    N      = EVEN NUMBER OF INPUT FUNCTION VALUES (MUST EXCEED 2)
C
C  OUTPUT:
C    AZ     = CONSTANT TERM IN SERIES
C    A      = (N/2-1) REAL OUTPUT VALUES OF COEFFICIENTS IN COS SERIES
C    B      = (N/2-1) REAL OUTPUT VALUES OF COEFFICIENTS IN SINE SERIES
C    AN     = COSINE(N/2*TK) TERM IN SERIES
C    YY     = DUMMY STORAGE OF LENGTH N+2 (REAL)
C    Z      = DUMMY STORAGE OF LENGTH 2*N (REAL)
C    W      = DUMMY STORAGE OF LENGTH N (REAL)
C  ************************************************************************
C            L=N/2-1
C     Y(K)=AZ+ SUM (A(L)*COS(L*TK)+B(L)*SIN(L*TK))+AN*COS(N/2*TK)
C              L=1
C  ************************************************************************
C
C  ROUTINES CALLED:
C    RFAST  - FAST FOURIER TRANSFORM OF REAL DATA
C
C  ROUTINES CALLED BY:
C    FOREGO - COMPUTES THE COEFFICIENTS OF THE FOURIER SERIES
C             REPRESENTATION OF R VS. ARC.  ONE LOBE OF A DIFFUSER CROSS
C             SECTION IS THUS APPROXIMATED FROM PHI=-THETA TO PHI=THETA.
C
C
C
      SUBROUTINE SERINV(Y,N,AZ,A,B,AN,YY,Z,W)
C
C  REVERSE OF 'SERIES'
C
C  INPUT:
C    Y(K)   = INPUT VALUE OF FUNCTION AT AN ANGLE OF TK=2.*PI*(K-1)/N
C               FOR K=1 TO K=N
C               PI = 3.1415927.....
C    N      = EVEN NUMBER OF INPUT FUNCTION VALUES (MUST EXCEED 2)
C
C  OUTPUT:
C    AZ     = CONSTANT TERM IN SERIES
C    A      = (N/2-1) REAL OUTPUT VALUES OF COEFFICIENTS IN COS SERIES
C    B      = (N/2-1) REAL OUTPUT VALUES OF COEFFICIENTS IN SINE SERIES
C    AN     = COSINE(N/2*TK) TERM IN SERIES
C    YY     = DUMMY STORAGE OF LENGTH N+2 (REAL)
C    Z      = DUMMY STORAGE OF LENGTH 2*N (REAL)
C    W      = DUMMY STORAGE OF LENGTH N (REAL
C
C  ROUTINES CALLED:
C    RFASTI - REVERSE OF 'RFAST'
C
C  ROUTINES CALLED BY:
C
```

```
C
      SUBROUTINE RFAST(X,Y,N,Z,W,S)
C
C  FAST FOURIER TRANSFORM OF REAL DATA
C
C  INPUT:
C    X       = N REAL INPUT VALUES
C    N       = EVEN NUMBER OF INPUT VALUES (MUST EXCEED 2)
C    S       = SIGN CONTROLLING DIRECTION OF TRANSFORM
C
C  OUTPUT:
C    Y       = N/2+1 COMPLEX OUTPUT VALUES
C    Z       = DUMMY STORAGE OF LENGTH 2N (REAL)
C    W       = DUMMY STORAGE OF LENGTH N (REAL)
C
C  THIS PRODUCES 'OUTPUT Y' FROM 'INPUT X', WHERE
C     ************************************************************************
C          K=N
C     Y(J)=SUM X(K)*EXP(SIGN(1.,S)*I*2*PI*(J-1)*(K-1)/N)
C          K=1
C     ************************************************************************
C  WITH I=SQRT(-1) AND PI=3.14159.....
C  NOTE THAT Y(N-J+2)=CONJ(Y(J)) FOR J=1 TO J=N/2+1
C  THUS ONLY Y(1) TO Y(N/2+1) ARE CALCULATED
C  COMPLEX NUMBERS ARE HANDLED IN FORTRAN 4 CONVENTION, NAMELY THE
C  REAL AND IMAGINARY PARTS ARE STORED IN ALTERNATE CELLS, STARTING
C  WITH THE REAL PART OF Y(1) IN THE FIRST LOCATION, ETC.
C
C  ROUTINES CALLED:
C    FAST   - FAST FOURIER TRANSFORM OF COMPLEX DATA
C
C  ROUTINES CALLED BY:
C    SERIES - DETERMINATION OF COEFFICIENTS IN A SERIES
C
```

```
C
      SUBROUTINE FAST (X,Y,N,Z,W,S)
C
C  FAST FOURIER TRANSFORM OF COMPLEX DATA
C
C  INPUT:
C    X       = N INPUT VALUES (COMPLEX)
C    N       = NUMBER OF VALUES
C
C  OUTPUT:
C    Y       = N OUTPUT VALUES (COMPLEX)
C    Z       = DUMMY STORAGE OF LENGTH 2N (COMPLEX)
C    W       = DUMMY STORAGE OF LENGTH N (COMPLEX)
C    S       = SIGN CONTROLLING DIRECTION OF TRANSFORM
C
C  THIS PRODUCES 'OUTPUT Y' FROM 'INPUT X', WHERE
C     ************************************************************************
C          K=N
C     Y(J)=SUM X(K)*EXP(SIGN(1.,S)*I*2*PI*(J-1)*(K-1)/N)
C          K=1
C     ************************************************************************
C  WITH I=SQRT(-1), S=+1. OR S=-1., AND PI=3.14159.....
C
C  ROUTINES CALLED:
C
C  ROUTINES CALLED BY:
C    RFAST  - FAST FOURIER TRANSFORM OF REAL DATA
C    RFASTI - REVERSE OF 'RFAST'
C
```

```
C
      SUBROUTINE EBC
C
C  CALCULATES THE POSITION OF THE DOWNSTREAM BOUNDARY AND THE DOWNSTREAM
C  MACH NUMBERS FOR EACH STREAM.
C
C  INPUT AERO DATA:
C    PT1, PT2, PINF, TT1, TT2, GAM1, GAM2, R1, R2
C
C  OUTPUT ARGUMENTS:
C    EM1S - PRIMARY STREAM MACH NO. FOR THE SPLITTER
C    EM2S - SECONDARY STREAM MACH NO. FOR THE SPLITTER
C
C  ROUTINES CALLED:
C    HAF  - SEARCH ROUTINE USED BY EBC
C
C  ROUTINES CALLED BY:
C    FLOMIX PROGRAM
C


      SUBROUTINE HAF(MAX,MIN,X,Y,IC,IER)
C
C  THIS ROUTINE IS A SEARCH ROUTINE FOR EBC.
C
C  INPUT ARGUMENTS:
C    MIN - MINIMUM VALUE OF OUTPUT PARAMETER FOR SEARCH
C    MAX - MAXIMUM VALUE OF OUTPUT PARAMETER FOR SEARCH
C    X   - CURRENT VALUE OF OUTPUT PARAMETER DURING SEARCH
C    Y   - INPUT PARAMETER TO BE MATCHED
C    IC  - 1, INPUT PARAMETER IS SPLITTER SECONDARY FLOW AREA
C        - 2, INPUT PARAMETER IS COMPOUND FLOW FUNCTION, BETA
C        - 3, INPUT PARAMETER IS SECONDARY FLOW RATE
C
C  OUTPUT ARGUMENTS:
C    X   - IC=1, OUTPUT PARAMETER IS SPLITTER STATIC PRESSURE
C        - IC=2, OUTPUT PARAMETER IS NOZZLE EXIT STATIC PRESSURE
C        - IC=3, OUTPUT PARAMETER IS DOWNSTREAM BOUNDARY STATIC PRESSURE
C    IER - ERROR INDICATOR; 0 IS O.K., 1 IS NO CONVERGENCE IN 20 TRIES.
C
C  ROUTINES CALLED:
C
C  ROUTINES CALLED BY:
C    EBC - CALCULATES THE POSITION OF THE DOWNSTREAM BOUNDARY AND THE
C          DOWNSTREAM MACH NUMBERS FOR EACH STREAM

C**********************************************************************
      SUBROUTINE GRID
C
C  THIS SUBROUTINE GENERATES A CARTESIAN MESH FOR THE DENSEST GRID.
C
C  ROUTINES CALLED:
C
C  ROUTINES CALLED BY:
C    FLOMIX PROGRAM
C
```

```
C*****************************************************************
      SUBROUTINE XRSUBS
C
C  THIS SUBROUTINE GENERATES COARSE GRID SUBSETS OF THE DENSEST GRID,
C  AS WELL AS CALCULATING COARSE GRID VALUES OF VARIABLES
C  SUCH AS IMAX, JMAX, IH, AND ITE.
C
C  ROUTINES CALLED:
C
C  ROUTINES CALLED BY:
C    FLOMIX PROGRAM
C

C*****************************************************************
      SUBROUTINE BCSETS(XNTR,RNTR,IMXINT)
C
C  THIS SUBROUTINE GENERATES THE ARRAYS WHICH ARE USED TO ESTABLISH THE
C  EXACT SURFACE BOUNDARY CONDITIONS.
C
C  OUTPUT ARGUMENTS:
C    XNTR   - X INTERPOLATED SURFACE COORDINATES FOR CPPLOT
C    RNTR   - R INTERPOLATED SURFACE COORDINATES FOR CPPLOT
C    IMXINT - NO. OF VALUES IN X AND R FOR EACH SURFACE
C
C  ROUTINES CALLED BY:
C    FLOMIX PROGRAM
C
C***********************************************
C            CONTOUR BOUNDARIES
C               L = 1 - CENTERBODY
C                 = 2 - INTERNAL SPLITTER
C                 = 3 - EXTERNAL SPLITTER
C                 = 4 - NOZZLE
C***********************************************
C


C*************************************************************
      SUBROUTINE PGUESS
C
C  THIS SUBROUTINE GENERATES AN INITIAL GUESS FOR THE POTENTIAL, PHI.
C  THE GUESS IS OBTAINED EITHER FROM A SAVED SOLUTION, THE
C  SOLUTION FROM THE PREVIOUS GRID, OR A GIVEN FUNCTIONAL FORM.
C
C  ROUTINES CALLED:
C
C  ROUTINES CALLED BY:
C  FLOMIX PROGRAM
C




      SUBROUTINE PLTGRD(XNTR,RNTR,IMXINT)
C
C     THIS ROUTINE HANDLES GRID PLOTTING
C
C     INPUT ARGUMENTS:
C       XNTR   - X INTERPOLATED SURFACE COORDINATES FROM BCSETS
C       RNTR   - R INTERPOLATED SURFACE COORDINATES FROM BCSETS
C       IMXINT - NO. OF VALUES IN X AND R FOR EACH SURFACE
C
C     ROUTINES CALLED:  PLTEK2
C
C     ROUTINES CALLED BY:  FLOMIX PROGRAM
C
```

```
C*****************************************************************
      SUBROUTINE INITL
C
C  THIS SUBROUTINE SETS UP INITIALIZATION FOR EXTRAPOLATED RELAXATION.
C
C  ROUTINES CALLED:
C
C  ROUTINES CALLED BY:
C    FLOMIX PROGRAM
C
C   1. IF AN EXTRAPOLATION DOES NOT OCCUR WITHIN INSTEP SWEEPS, AN
C      EXTRAPOLATION WILL BE FORCED. AT THIS POINT A NEW TOLJMP
C      COEFFICIENT WILL ALSO BE COMPUTED.
C   2. IXTRAP - A SWEEP COUNTER FOR COMPARISON WITH INSTEP
C   3. AT LEAST INDJMP SWEEPS WILL OCCUR BETWEEN EXTRAPOLATIONS.
C   4. TOLJMP - A COEFFICIENT WHICH IS MULTIPLIED BY THE STANDARD
C      DEVIATION OF THE DISTRIBUTION OF CORRECTIONS OVER THE MATRIX FOR
C      A GIVEN SWEEP.
C      THE ABS. VALUE OF THE AVERAGE CORRECTION IS COMPARED WITH TOLJMP
C      TIMES THE STANDARD DEVIATION.
C   5. NSTEPS - THE NUMBER OF NODES IN THE GRID.
C      CALCULATIONS.
C   6. XLAMS  - THE SUM OF THE RATIOS OF THE CORRECTIONS WITHIN EACH
C      SWEEP.
C   7. RLAMSS - THE SUM OF THE SQUARES OF THE RATIOS OF THE CORRECTIONS
C      WITHIN ANY GIVEN SWEEP.
C   8. RLAMS  - THE SUM OF THE CORRECTIONS OVER ANY GIVEN SWEEP.
C   9. ISTEP  - A COUNTER WHICH IS COMPARED WITH INDJMP AND RESET TO 1
C      WHEN AN EXTRAPOLATION TAKES PLACE.
C  10. NSWAVE - THE NUMBER OF SWEEPS USED IN CALCULATING THE AVERAGE
C      RESIDUAL FOR AN EXTRAPOLATION.
C  11. ISWAVE  - A COUNTER FOR COMPARISON WITH NSWAVE.
C

C*****************************************************************
      SUBROUTINE SLOR
C
C  THIS SUBROUTINE PERFORMS A SUCCESSIVE LINE OVER-RELAXATION. FOR
C  EACH COLUMN IN THE CARTESIAN MESH, A TRIDIAGONAL MATRIX
C  IS SET UP AND SOLVED. THE CORRECTIONS ARE APPLIED WITH
C  AN OVER-RELAXATION FACTOR FOR SUBSONIC FLOW, AND AN
C  UNDER-RELAXATION FACTOR FOR SUPERSONIC FLOW. WHEN
C  THE PROPER CRITERIA ARE MET, AN EXTRAPOLATION IS CALLED.
C
C  ROUTINES CALLED:
C    MATRIX - SETS UP THE MATRIX OF COEFFICIENTS RESULTING
C             FROM THE PARTIAL DIFFERENTIAL EQUATION AND THE BOUNDARY
C             CONDITIONS. THE R*PHIR RULE FOR THE CENTERBODY AND THE
C             OUTER BOUNDARY IS INCLUDED IN THE MATRIX TO SIMPLIFY THE
C             LOGIC FOR VARIABLE COLUMN LENGTHS. AT SOME FUTURE DATE
C             IT MAY BE CHANGED FOR THE SAKE OF EFFICIENCY.
C    TRIDI  - SOLVES A SET OF N TRIDIAGONAL EQUATIONS AS OBTAINED IN
C             THE MAIN PROGRAM FOR A RADIAL COLUMN.
C
C  ROUTINES CALLED BY:
C    FLOMIX PROGRAM
C

C*****************************************************************
      SUBROUTINE FARFLD
C
C  THIS SUBROUTINE GENERATES THE FAR FIELD BOUNDARY CONDITIONS. IT IS
C  INCLUDED IN THE RELAXATION SWEEPING LOOP TO ALLOW FOR PERIODIC
C  UPDATING BASED ON THE CIRCULATION.
C
C  ROUTINES CALLED:
C
C  ROUTINES CALLED BY:
C    FLOMIX PROGRAM
```

```
C*************************************************************
      SUBROUTINE MATRIX
C
C  THIS SUBROUTINE SETS UP THE MATRIX OF COEFFICIENTS RESULTING
C  FROM THE PARTIAL DIFFERENTIAL EQUATION AND THE BOUNDARY
C  CONDITIONS. THE R*PHIR RULE FOR THE CENTERBODY AND THE
C  OUTER BOUNDARY IS INCLUDED IN THE MATRIX TO SIMPLIFY THE
C  LOGIC FOR VARIABLE COLUMN LENGTHS. AT SOME FUTURE DATE
C  IT MAY BE CHANGED FOR THE SAKE OF EFFICIENCY.
C
C  ROUTINES CALLED:
C    BCABCW - ESTABLISHES BOUNDARY CONDITION VALUES FOR MATRIX
C             COEFFICIENTS A, B, C, AND W
C    PDEABC - CALCULATES THE PDE MATRIX COEFFICIENTS A,B, & C, AND THE
C             RIGHT HAND SIDE W
C
C  ROUTINES CALLED BY:
C    SLOR   -  PERFORMS A SUCCESSIVE LINE OVER-RELAXATION. FOR
C              EACH COLUMN IN THE CARTESIAN MESH, A TRIDIAGONAL MATRIX
C              IS SET UP AND SOLVED. THE CORRECTIONS ARE APPLIED WITH
C              AN OVER-RELAXATION FACTOR FOR SUBSONIC FLOW, AND AN
C              UNDER-RELAXATION FACTOR FOR SUPERSONIC FLOW. WHEN
C              THE PROPER CRITERIA ARE MET, AN EXTRAPOLATION IS CALLED.

C*************************************************************
      SUBROUTINE TRIDI(A,B,C,VECTOR,W,N)
C
C  THIS SUBROUTINE SOLVES A SET OF N TRIDIAGONAL EQUATIONS AS
C  OBTAINED IN THE MAIN PROGRAM FOR A RADIAL COLUMN.  THE RESULTS
C  ARE LEFT IN THE ARRAY *VECTOR* AND A,B,C AND W ARE DESTROYED.
C
C  INPUT:
C    A      - WORK VECTOR FOR TRIDIAGONAL EQUATIONS
C    B      - WORK VECTOR FOR TRIDIAGONAL EQUATIONS
C    C      - WORK VECTOR FOR TRIDIAGONAL EQUATIONS
C    W      - WORK VECTOR FOR TRIDIAGONAL EQUATIONS
C    N      - NO. OF TRIDIAGONAL EQUATIONS
C
C  OUTPUT:
C    VECTOR - RESULTING ARRAY
C
C  ROUTINES CALLED:
C
C  ROUTINES CALLED BY:
C    SLOR   - PERFORMS A SUCCESSIVE LINE OVER-RELAXATION. FOR
C             EACH COLUMN IN THE CARTESIAN MESH, A TRIDIAGONAL MATRIX
C             IS SET UP AND SOLVED. THE CORRECTIONS ARE APPLIED WITH
C             AN OVER-RELAXATION FACTOR FOR SUBSONIC FLOW, AND AN
C             UNDER-RELAXATION FACTOR FOR SUPERSONIC FLOW. WHEN
C             THE PROPER CRITERIA ARE MET, AN EXTRAPOLATION IS CALLED.

C*************************************************************
      SUBROUTINE RESCLI
C
C  THIS SUBROUTINE CALCULATES RESIDUES FOR EACH SWEEP THROUGH RELAXATION
C  LOOP.
C
C  ROUTINES CALLED:

C    MATRIX - SETS UP THE MATRIX OF COEFFICIENTS RESULTING
C             FROM THE PARTIAL DIFFERENTIAL EQUATION AND THE BOUNDARY
C             CONDITIONS. THE R*PHIR RULE FOR THE CENTERBODY AND THE
C             OUTER BOUNDARY IS INCLUDED IN THE MATRIX TO SIMPLIFY THE
C             LOGIC FOR VARIABLE COLUMN LENGTHS. AT SOME FUTURE DATE
C             IT MAY BE CHANGED FOR THE SAKE OF EFFICIENCY.
C
C  ROUTINES CALLED BY:
C    FLOMIX PROGRAM
C
```

```
C*************************************************************
      SUBROUTINE PDEABC(ISTR)
C
C  THIS SUBROUTINE CALCULATES THE PARTIAL DIFFERENTIAL EQUATION
C  MATRIX COEFFICIENTS, A,B, AND C, AND THE
C  RIGHT HAND SIDE, W.
C
C  ROUTINES CALLED:
C
C  ROUTINES CALLED BY:
C    MATRIX - SETS UP THE MATRIX OF COEFFICIENTS RESULTING
C             FROM THE PARTIAL DIFFERENTIAL EQUATION AND THE BOUNDARY
C             CONDITIONS. THE R*PHIR RULE FOR THE CENTERBODY AND THE
C             OUTER BOUNDARY IS INCLUDED IN THE MATRIX TO SIMPLIFY THE
C             LOGIC FOR VARIABLE COLUMN LENGTHS. AT SOME FUTURE DATE
C             IT MAY BE CHANGED FOR THE SAKE OF EFFICIENCY.
C
C*************************************************************
      SUBROUTINE BCABCW(ISTR,IBND)
C
C  THIS SUBROUTINE ESTABLISHES BOUNDARY CONDITION VALUES FOR MATRIX
C  COEFFICIENTS A, B, C, AND W
C
C  INPUT ARGUMENTS:
C    ISTR - STREAM NUMBER   (1-PRIMARY, 2-SECONDARY)
C    IBND - BOUNDARY NUMBER (1-CENT.,2-INNER SPL.,3-OUTER SPL.,4-NOZZLE)
C
C  ROUTINES CALLED:
C    DELTAF - CALCULATES DELTA FUNCTIONS
C
C  ROUTINES CALLED BY:
C    MATRIX - SETS UP THE MATRIX OF COEFFICIENTS RESULTING
C             FROM THE PARTIAL DIFFERENTIAL EQUATION AND THE BOUNDARY
C             CONDITIONS. THE R*PHIR RULE FOR THE CENTERBODY AND THE
C             OUTER BOUNDARY IS INCLUDED IN THE MATRIX TO SIMPLIFY THE
C             LOGIC FOR VARIABLE COLUMN LENGTHS. AT SOME FUTURE DATE
C             IT MAY BE CHANGED FOR THE SAKE OF EFFICIENCY.
C
C*************************************************************
      SUBROUTINE PLUME
C
C  THIS SUBROUTINE IS USED FOR CONFIGURING THE PLUME.
C
C  ROUTINES CALLED:
C
C  ROUTINES CALLED BY:
C    MATRIX - SETS UP THE MATRIX OF COEFFICIENTS RESULTING
C             FROM THE PARTIAL DIFFERENTIAL EQUATION AND THE BOUNDARY
C             CONDITIONS. THE R*PHIR RULE FOR THE CENTERBODY AND THE
C             OUTER BOUNDARY IS INCLUDED IN THE MATRIX TO SIMPLIFY THE
C             LOGIC FOR VARIABLE COLUMN LENGTHS. AT SOME FUTURE DATE
C             IT MAY BE CHANGED FOR THE SAKE OF EFFICIENCY.
C

      SUBROUTINE UPDATE
C
C  THIS SUBROUTINE CALCULATES THE CORRECTIONS FOR THE NEXT SWEEP.
C
C  ROUTINES CALLED:
C    EXTRAP - CALCULATES THE EXTRAPOLATED RELAXATION FOR THE NEXT SWEEP
C
C  ROUTINES CALLED BY:
C    FLOMIX  PROGRAM
C


      SUBROUTINE EXTRAP
C
C  THIS SUBROUTINE CALCULATES THE EXTRAPOLATED RELAXATION FOR THE NEXT
C  SWEEP.
C
C  ROUTINES CALLED:
C
C  ROUTINES CALLED BY:
C    UPDATE - CALCULATES THE CORRECTIONS FOR THE NEXT SWEEP
C
```

```
C*************************************************************
      FUNCTION DELTAF(I,J)
C
C   THIS FUNCTIONS IS USED BY BCABCW TO CALCULATE DELTA FUNCTIONS.
C
C   ROUTINES CALLED BY:
C     BCABCW - ESTABLISHES BOUNDARY CONDITION VALUES FOR MATRIX
C              COEFFICIENTS A, B, C, AND W
C
C-------------------------------------------------------------

C*************************************************************
      SUBROUTINE OUTPUT(XNTR,RNTR,IMXINT)
C
C  THIS SUBROUTINE CALLS THE VARIOUS OUTPUT SUBROUTINES THAT APPLY TO
C  EACH GRID.
C
C  INPUT ARGUMENTS:
C    XNTR   - X INTERPOLATED SURFACE COORDINATES FROM BCSETS
C    RNTR   - R INTERPOLATED SURFACE COORDINATES FROM BCSETS
C    IMXINT - NO. OF VALUES IN X AND R FOR EACH SURFACE
C
C  ROUTINES CALLED:
C    MASFLO - PERFORMS THE MASS FLOW INTEGRATIONS
C    CPPLOT - PLOTS CP CALCULATIONS
C    FLDPLT - PLOTS CPS IN THE FLOW AREA
C
C  ROUTINES CALLED BY:
C    FLOMIX PROGRAM
C

C*************************************************************
      SUBROUTINE PHIPLT(PHI,X,R,IMAX,JMAX,NI,NJ,NK,K,IC,D,H,UP,SHR,ETA)
C
C     THIS ROUTINE HANDLES PLOTTING OF PHI VALUES.
C
C     ROUTINES CALLED:  PLTEK2
C
C     ROUTINES CALLED BY:
C

C*************************************************************
      SUBROUTINE CPPLOT(XNTR,RNTR,IMXINT)
C
C     THIS ROUTINE PLOTS CP CALCULATIONS
C
C     INPUT ARGUMENTS:
C       XNTR   - X INTERPOLATED SURFACE COORDINATES FROM BCSETS
C       RNTR   - R INTERPOLATED SURFACE COORDINATES FROM BCSETS
C       IMXINT - NO. OF VALUES IN X AND R FOR EACH SURFACE
C
C     ROUTINES CALLED:  PLTEK2, MVCHAR
C
C     ROUTINES CALLED BY:
C       OUTPUT - CALLS THE VARIOUS OUTPUT SUBROUTINES THAT APPLY
C                TO EACH GRID. THESE INCLUDE THE CP PLOTS, THE MASS
C                FLOW INTEGRATIONS, AND THE DRAG CALCULATION.
C

C*************************************************************
      SUBROUTINE FLDPLT
C
C   PLOTS CPS IN THE FLOW AREA
C
C   ROUTINES CALLED BY:
C     OUTPUT - CALLS THE VARIOUS OUTPUT SUBROUTINES THAT APPLY TO EACH
C              GRID
```

```
C*****************************************************************
      SUBROUTINE RECOMB(THE,CPS,IMXINT,NEXT)
C
C  THIS ROUTINE COMBINES EACH HARMONIC SOLUTION INTO ONE SOLUTION.
C
C  INPUT ARGUMENTS:
C    THE    - THETA ANGLES
C    CPS    - CPS FOR EACH CONTOUR
C    IMXINT - NO. OF VALUES IN EACH CONTOUR
C    NEXT   - NO. OF EXTERNAL SPLITTER STATIONS
C
C  ROUTINES CALLED BY:
C    FLOMIX PROGRAM
C


C*****************************************************************
      SUBROUTINE PJMPLT(PJMPTT,RMXPTT,RAVPTT,IMXRSP,JMXRSP,NSTOT,NHARM)
C
C     THIS ROUTINE HANDLES PLOTTING OF THE JUMP IN PHI VALUES AND THE
C     MAXIMUM AND AVERAGE RESIDUALS.
C
C     INPUT ARGUMENTS:
C       PJMPTT - JUMP IN PHI VALUES
C       RMXPTT - MAXIMUM RESIDUALS
C       RAVPTT - AVERAGE RESIDUALS
C       IMXRSP - MAXIMUM RESIDUAL POINTER FOR EACH SWEEP FOR I
C       JMXRSP - MAXIMUM RESIDUAL POINTER FOR EACH SWEEP FOR J
C       NSTOT  - MAXIMUM NO. OF POINTS TO PLOT
C       NHARM  - NO. OF HARMONICS(MODES)
C
C     ROUTINES CALLED:  PLTEK2
C
C     ROUTINES CALLED BY:  FLOMIX PROGRAM
C
```

REFERENCES

1. Kuchar, A.P. and Chamberlin, R., "Scale Model Performance Test Investigation of Exhaust System Mixes for an Energy Efficient Engine (E^3) Propulsion System, "AIAA Paper 80-0229, AIAA 18th Aerospace Sciences Meeting, Pasadena, Ca., 1980.

2. Kuchar, A.P. and Chamberlin, R., "Scale Model Performance Test Investigation of Mixed Flow Exhaust Systems for an Energy Efficient Engine (E^3) Propulsion System, "AIAA Paper 83-0541, AIAA 21st Aerospace Sciences Meeting, Pasadena, Ca., 1983.

3. Kozlowski, H. and Kraft, G. "Experimental Evaluation of Exhaust Mixers for an Energy Efficient Engine, "AIAA Paper 80-1088, AIAA 18th Aerospace Sciences Meeting, Pasadena, Ca., 1980.

4. Paterson, R. W. and Werle, M. J., "Turbofan Forced Mixer Flow Field", United Tech. Res. Center, UTRC/R79-912924, 1979.

5. Paterson, R. W., "Turbo Forced Mixer - Nozzle Internal Flowfield, I - A Benchmark Experimental Study", NASA CR3492, 1982.

6. Anderson, B. H., Povinelli, L.A., and Gerstenmaier, W. G., "Influence of Pressure Driven Secondary Flows of the Behavior of Turbofan Forced Mixers", AIAA Paper 80-1198, AIAA 18th Aerospace Sciences Meeting, Pasadena, Ca., 1980.

7. Anderson, B. H. and Povinelli, L.A., "Factors Which Influence The Behavior of Turbofan Forced Mixer Nozzles", AIAA Paper 81-0274, AIAA 19th Aerospace Sciences Meeting, St. Louis, MO., 1981.

8. Golden, D. P., Barber, T. J. and Chin, W. C., "An Axisymmetric Nacelle and Turboprop inlet Analysis including Power Simulation," J. Aircraft, Vol. 20, No. 6, 1983, p 536.

9. Wedan, B., and South, J.C., "A Method for Solving the Transonic Full Potential Equation for General Configurations, "AiAA Pages 83-1889, AIAA 6th Computational Fluid Dynamics Conference, Danver, MA, 1983.

10. Bernstein, A., Heiser, W. and Hevenor, C., "Compound Compressible Nozzle Flow," Trans. ASME SERIES E, J. Appl. Mech., 3, 1967, pp. 549-54.

11. Amiet, R. K., Users Manual for Task I - Laterally Planar Inviscid Mixer Analysis. PWA-5904-18, 1983.

12. Kozlowski, H., and Larkin, M., Energy Efficient Engine Exhaust Mixer Model Technology Report. NASA CR-165459 (PWA-5594-164), 1981.

13. Larkin, M. J.,, and Blatt, J. R., Energy Efficient Engine Exhaust Mixer Model Technology Report Addendum - Phase III Test Report. NASA CR to be issued, PWA-5594-271, 1984.

14. Spreiter, J. R., Aerodynamics of Wings and Bodies at Transonic Speeds. J.A.S., Vol. 26, No. 8, 1959, pp. 465-487.

15. Malmuth, N. D., An Asymptotic Theory of Wind Tunnel Wall Interference on Subsonic Slender Bodies. AIAA Paper No. 84-1625, AIAA 17th Fluid Dynamics, Plasma Dynamics and Lasers Conference, Snowmass, CO, 1984.

APPENDIX

Scarf Angle Analysis

Mixing performance has been found to depend on the geometry characteristics of the lobe trailing edge plane. In particular, cutback or scarfing can be used to optimize mixer performance. Typically , the scarf angle (ς) can vary $\pm$ 15° from a radial cut. Analysis of such configurations is complicated by the irregular radial surface presented when viewed in a cylindrical frame of reference. An alternate representation, using a skewed system aligned to the lobe trailing edge avoids this problem.

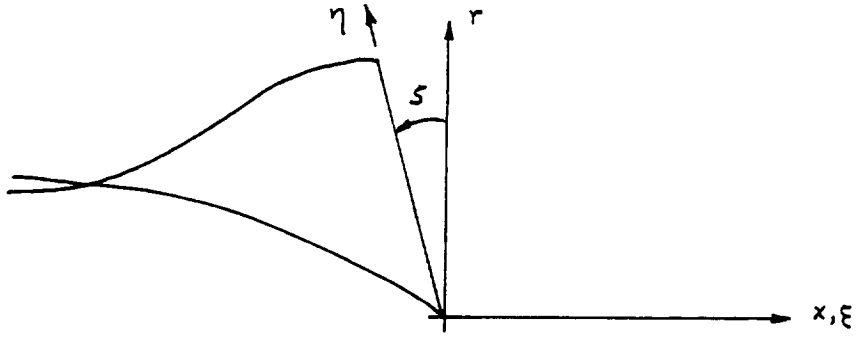

The governing equations can be transformed from the physical (x,r) to the computational plane (ξ,η) by means of the following transformation.

$$\xi = x - \Lambda r \qquad \eta = \frac{r}{c} \tag{A.1}$$

where $\Lambda = \tan\varsigma$ =constant and $c = \cos\varsigma$ = constant. The local velocities can then be related to these coordinates through chain rule differentiation.

$$\frac{\partial}{\partial x}(\ ) = \frac{\partial \xi}{\partial x}\frac{\partial}{\partial \xi}(\ ) + \frac{\partial \eta}{\partial x}\frac{\partial}{\partial \eta}(\ ) = \frac{\partial}{\partial \eta}(\ ) \tag{A.2a}$$

$$\frac{\partial}{\partial r}(\ ) = \frac{\partial \xi}{\partial r}\frac{\partial}{\partial \xi}(\ ) + \frac{\partial \eta}{\partial r}\frac{\partial}{\partial \eta}(\ ) = -\Lambda\frac{\partial}{\partial \xi}(\ ) + \frac{1}{c}\frac{\partial}{\partial \eta}(\ ) \tag{A.2b}$$

or

$$\beta^2 q_x = \beta^2 q_\xi \quad \& \quad q_r = -\Lambda\beta^2 q_\xi + \frac{1}{c} q_\eta \tag{A.3}$$

The β^2 term has been introduced to reflect the comprisable term from the s.d.t. expansion. Applying these flux definitions to a balance over a general element, in a cylindrical mesh, yields

$$\int_{E-W} (\beta^2 g_{x_k})\, r\,dr - \int_{E-W} g_{r_k}\, r\,dx + \int_{N-S} g_{r_k}\, r\,dx - K^2 \int_{\Delta\theta} g_k \frac{dA}{r} = 0 \qquad (A.4)$$

Discriticizing reduces (A.4) to

$$\left[\beta^2 g_{x_{kE}}\, c\, A_E - \beta^2 g_{x_{kW}}\, c\, A_W\right] - \left[g_{r_{kE}}\, s\, A_E - g_{r_{kW}}\, s\, A_W\right]$$

$$+ g_{r_{kN}} A_N - g_{r_{kS}} A_S - \frac{K^2}{r} g_k \Delta A = 0, \qquad (A.5)$$

where g_x, g_r are differenced along the mesh when expressed in terms of (A.3). Similarly one can treat boundary intersecting elements in this skewed system. Recalling equation (22)

$$\int_{E-W} \beta^2 g_{x_k}\, r\,dr + \int_{N-S} g_{r_k}\, r\,dx - \int_{Rm} \bar{g}_{r_k}\, r\,dx - K^2 \int_{\Delta\theta} g_k \frac{dA}{r} = 0$$

where

$$\bar{g}_{r_k} = \lambda'_k + G(\lambda_m, g_m)$$

is the "known" surface flux along the main surface Rm (x). The flux balance in the skewed system becomes

$$\left[A.5\right] - R_m \Delta x\, \bar{g}_{r_k} = 0$$

where the local are as again represent only the exposed portion of the cell.

It is desirable, in general, to have a skewed radial mesh over the entire calculation domain but boundary conditions are typically defined along radial upstream and downstream planes. The skewing transformation (A.1) must consider $\Lambda=\Lambda(x,r)$. A generalization of the previous analysis is simplified if we introduce the flux balance in terms of the contravariant velocity components; those defined normal to the (ξ,η) coordinates. Following the approach of Doria, equations (A.2) applied to (x,r) yields four separate equation systems for the transformation metrics; eq.

$$(\quad)_x \longrightarrow \begin{cases} 1 = \xi_x x_\xi + \eta_x x_\eta \\ 0 = \xi_r x_\xi + \eta_r x_\xi \end{cases} \qquad x_\xi = \frac{\eta_r}{\xi_x \eta_r - \eta_x \xi_r} = 1$$

If Λ = constant, these equations yield the following metrics relations

$$x_\xi = 1 \quad x_\eta = S \quad r_\xi = 0 \quad r_\eta = C \tag{A.6}$$

Associated with this transformation are the Jacobian

$$J = x_\xi r_\eta - x_\eta r_\xi = C \tag{A.7a}$$

and the three invariant components of the metric tensor

$$\begin{aligned} a_{11} &= x_\xi^2 + r_\xi^2 = 1 \\ a_{12} &= x_\xi x_\eta + r_\xi r_\eta = 0 \\ a_{22} &= x_\eta^2 + r_\eta^2 = 1 \end{aligned} \tag{A.7b}$$

The conservation flux balance, in terms of the contravariant velocities (U,V) associated with (ξ,η) directions, is now given by the following components

$$JUA_\xi = r_\xi A_\xi + \frac{A_\xi}{J}\left[a_{22}\beta^2 q_\xi - a_{12} q_\eta\right] = r_\eta A_\xi + A_\xi\left[\frac{\beta^2}{C} q_\xi - \Lambda q_\eta\right]$$

$$JVA_\eta = -r_\xi A_\eta + \frac{A_\eta}{J}\left[-a_{12}\beta^2 q_\xi + a_{11} q_\eta\right] = -r_\xi A_\eta + A_\eta\left[\right. \tag{A.8}$$

$$\left. -\beta^2 q_\xi \Lambda + \frac{q_\eta}{C}\right]$$

The leading term in each expression reflects the contribution of the freestream velocity in the x-aligned perturbation potential formulation. One can compare (A.8) and (A.5) to check for consistency of the models.

$$\begin{cases} g_{r_N} A_N = \left[-\Lambda\beta^2 g_\xi + \frac{1}{c} g_\eta \right]_N A_N \\ \left[J \vee A_\eta \right]_N = A_N \left[-\Lambda\beta^2 g_\xi + \frac{1}{c} g_\eta \right]_N \end{cases}$$

$$\begin{cases} \left(\beta^2 g_x c - g_r s \right)_w A_w = A_w \left[\beta^2 c g_\xi - s\left(-\beta^2 \Lambda g_\xi + \frac{1}{c} g_\eta \right) \right]_w = A_w \left(\frac{\beta^2}{c} g_\xi - \Lambda g_\eta \right)_w \\ \left(J \cup A_\xi \right)_w = A_w \left[\frac{\beta^2}{c} g_\xi - \Lambda g_\eta \right]_w \end{cases}$$

In the above analysis the freestream component is neglected. For a general element it will cancel out with the opposing face's contribution. Special consideration is needed for the surface intersecting case.

The previous analysis can now be extended to include problems to wherein the mesh skewing varies.

$$\xi = x - \Lambda(x,r)\, r$$

$$\eta = \frac{r}{c(x,r)}$$

The metric invariants and Jacobian (A.7a,b) can be reevaluated in terms of

$$\xi_x = 1 - \frac{r}{c} \frac{\partial \Lambda}{\partial x} \qquad \xi_r = -\Lambda - \frac{r}{c^2} \frac{\partial \Lambda}{\partial r}$$

$$\eta_x = \frac{\Lambda}{c} \frac{\partial \Lambda}{\partial x} \qquad \eta_r = \frac{1}{c} + \frac{\Lambda}{c} \frac{\partial \Lambda}{\partial r}$$

The exact relationship for ζ, C, Λ can be obtained as follows. Consider the mesh generated from the lobe trailing edge to some downstream phase. Generate mesh skewing from fan valley contour.

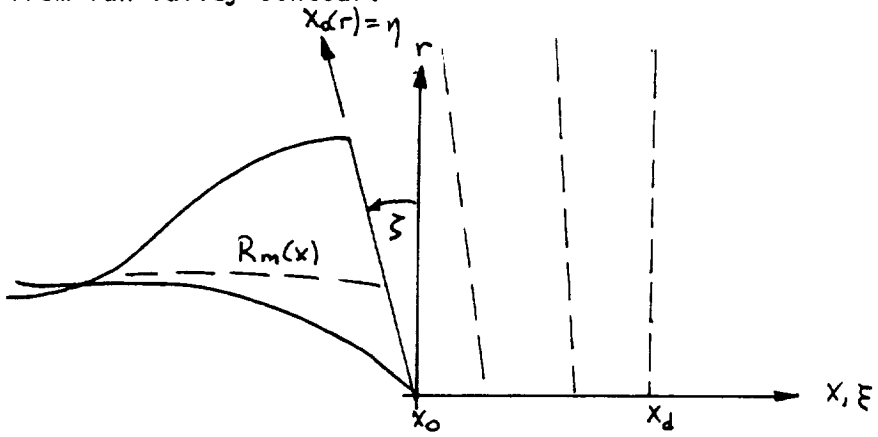

The equation of the lobe trailing edge is

$$X_o(r) = X_o(r_o) + (r - r_o)\,\Lambda_o^{-1}$$

Similarly the downstream mesh boundary is given by

$$X_d(r) = X_d$$

Linearly adjusting between these boundaries

$$\lambda = \left(\frac{X - X_o(r)}{X_d - X_o(r)}\right) = \frac{X_o(\lambda) - X_o(r_o)}{X_d - X_o(r_o)}$$

one obtains a general function expression for the x grid variation

$$X(\lambda) = (1-\lambda)X_o(r) + \lambda X_d$$

In this frame Λ, at any η line, is given by

$$\Lambda(\lambda) = \Lambda(x,r) = \frac{(r - r_o)}{\left[X(\lambda) - X(r_o)\right]}$$

NASA
National Aeronautics and Space Administration

Report Documentation Page

1. Report No.	2. Government Accession No.	3. Recipient's Catalog No.
NASA CR-4147		

4. Title and Subtitle	5. Report Date
Turbofan Forced Mixer Lobe Flow Modeling II - Three-Dimensional Inviscid Mixer Analysis (FLOMIX)	October 1988
	6. Performing Organization Code

7. Author(s)	8. Performing Organization Report No.
T. Barber	None (E-4084)
	10. Work Unit No.
	505-62-21

9. Performing Organization Name and Address	11. Contract or Grant No.
United Technologies Corporation Pratt & Whitney Engineering Division East Hartford, Connecticut	NAS3-23039
	13. Type of Report and Period Covered Contractor Report Final
12. Sponsoring Agency Name and Address	14. Sponsoring Agency Code
National Aeronautics and Space Administration Lewis Research Center Cleveland, Ohio 44135-3191	

15. Supplementary Notes

Project Manager, Allan R. Bishop, Internal Fluid Mechanics Division, NASA Lewis Research Center.

16. Abstract

A three-dimensional potential analysis (FLOWMIX) has been formulated and applied to the inviscid flow over a turbofan forced mixer. The method uses a unique small disturbance formulation to analytically uncouple the circumferential flow from the radial and axial flow problem, thereby reducing the analysis to the solution of a series of axisymmetric problems. These equations are discretized using a flux volume formulation along a Cartesian grid. The method extends earlier applications of the Cartesian method to complex cambered geometries. The effects of power addition are also included within the potential formulation. Good agreement is obtained with an alternate small disturbance analysis for a "high penetration" symmetric mixer in a planar duct. In addition, calculations showing pressure distributions and induced secondary vorticity fields are presented for practical turbofan mixer configurations, and where possible, comparison has been made with available experimental data. A detailed description of the required data input and coordinate definition is presented along with a sample data set for a practical forced mixer configuration. A brief description of the program structure and subroutines is also provided.

17. Key Words (Suggested by Author(s))	18. Distribution Statement
Mixers Lobe flow modeling Three-dimensional flows	Unclassified - Unlimited Subject Category 02

19. Security Classif. (of this report)	20. Security Classif. (of this page)	21. No of pages	22. Price*
Unclassified	Unclassified	76	A05

*For sale by the National Technical Information Service, Springfield, Virginia 22161

National Aeronautics and
Space Administration
Code NTT-4

Washington, D.C.
20546-0001